Deciphering the *Physalis floridana Double-Layered-Lantern1* Mutant Provides Insights into Functional Divergence of the *GLOBOSA* Duplicates within the Solanaceae[1][C][W]

Ji-Si Zhang[2], Zhichao Li[2], Jing Zhao, Shaohua Zhang, Hui Quan, Man Zhao, and Chaoying He*

State Key Laboratory of Systematic and Evolutionary Botany, Institute of Botany, Chinese Academy of Sciences, Nanxincun 20, Xiangshan, Haidian, 100093 Beijing, China (J.-S.Z., Z.L., J.Z., S.Z., H.Q., M.Z., C.H.); and University of Chinese Academy of Sciences, Yuquan Road 19, 100049 Beijing, China (J.-S.Z., Z.L., J.Z., S.Z., H.Q., M.Z.)

ORCID ID: 0000-0002-2550-0170 (C.H.).

Physalis spp. develop the "Chinese lantern" trait, also known as inflated calyx syndrome, that is a morphological novelty. Here, we identified the *double-layered-lantern1* (*doll1*) mutant, a recessive and monofactorial mutation, in *Physalis floridana*; its corolla and androecium were transformed into the calyx and gynoecium, respectively. Two *GLOBOSA*-like MADS-box paralogous genes *PFGLO1* and *PFGLO2* were found in *Physalis floridana*, while the mutated phenotype was cosegregated with a large deletion harboring *PFGLO1* and was complemented by the *PFGLO1* genomic locus in transgenic plants, and severe *PFGLO1* knockdowns phenocopied *doll1*. Thus, *DOLL1* encodes the PFGLO1 protein and plays a primary role in determining corolla and androecium identity. However, specific *PFGLO2* silencing showed no homeotic variation but rather affected pollen maturation. The two genes featured identical floral expression domains, but the encoding proteins shared 67% identity in sequences. PFGLO1 was localized in the nucleus when expressed in combination with a DEFICIENS homolog from *Physalis floridana*, whereas PFGLO2 was imported to the nucleus on its own. The two proteins were further found to have evolved different interacting partners and regulatory patterns, supporting the hypothesis that PFGLO2 is functionally separated from organ identity. Such a divergent pattern of duplicated *GLO* genes is unusual within the Solanaceae. Moreover, the phenotypes of the *PFGLO1PFGLO2* double silencing mutants suggested that *PFGLO2*, through genetically interacting with *PFGLO1*, also exerts a role in the control of organ number and tip development of the second floral whorl. Our results, therefore, shed new light on the functional evolution of the duplicated *GLO* genes.

Morphological diversification is usually accompanied by an increase in the complexity of genetic material. The process is often achieved through gene duplication events that can provide the raw material for diversification and enable a sort of playground from which novelties of gene structures, protein function, and orgamismal morphology can emerge during evolution (Irish and Litt, 2005; Freeling and Thomas, 2006). However, the genetic architectures of the morphological diversification and the emergence of morphological novelty remain largely unknown. Nonetheless, in these evolutionary processes, it is assumed that processes such as gene expression, protein-protein interactions, and regulation targets of the orthologous genes or the duplicated genes can be altered. These dynamic processes lead to subfunctionalization, neofunctionalization, or loss of genes, thus bringing about morphological innovation (Irish and Litt, 2005; Zhao et al., 2013). The "Chinese lantern," also called inflated calyx syndrome (ICS) in *Physalis* spp., is a morphological novelty within the Solanaceae (Fig. 1A; He and Saedler, 2005). The trait is triggered by fertilization and is controlled by action of hormones (He and Saedler, 2005, 2007). Furthermore, the molecular genetic basis underlying the origin of this novel trait has started to be empirically deciphered (He and Saedler, 2005, 2007; He et al., 2007; Zhao et al., 2013). The MADS-box gene2 from *Physalis floridana* (*MPF2*) belongs to a small subfamily of the MADS-box genes (He and Saedler, 2005). Heterotopic expression of *MPF2* is key to the origin of ICS; the gene mainly controls ICS size (He and Saedler, 2005, 2007). The second functionally characterized MADS-box protein associated with the development of ICS was MPF3 (encoded by *MPF3*, the MADS-box gene3 from *Physalis floridana*), the euAP1 ortholog of APETALA1 (AP1) in Arabidopsis (*Arabidopsis thaliana*), and SQUAMOSA (SQUA) in *Antirrhinum majus* (Huijser et al., 1992; Mandel et al., 1992; Zhao et al., 2013). MPF3 exerts its role in the development

[1] This work was supported by grants from the National Natural Science Foundation of China (nos. 31070203 and 30870175), by the Hundred Talent Program of the Chinese Academy of Sciences, and by a grant from the Education Ministry of China.

[2] These authors contributed equally to the article.

* Address correspondence to chaoying@ibcas.ac.cn.

The author responsible for distribution of materials integral to the findings presented in this article in accordance with the policy described in the Instructions for Authors (www.plantphysiol.org) is: Chaoying He (chaoying@ibcas.ac.cn).

[C] Some figures in this article are displayed in color online but in black and white in the print edition.

[W] The online version of this article contains Web-only data.

www.plantphysiol.org/cgi/doi/10.1104/pp.113.233072

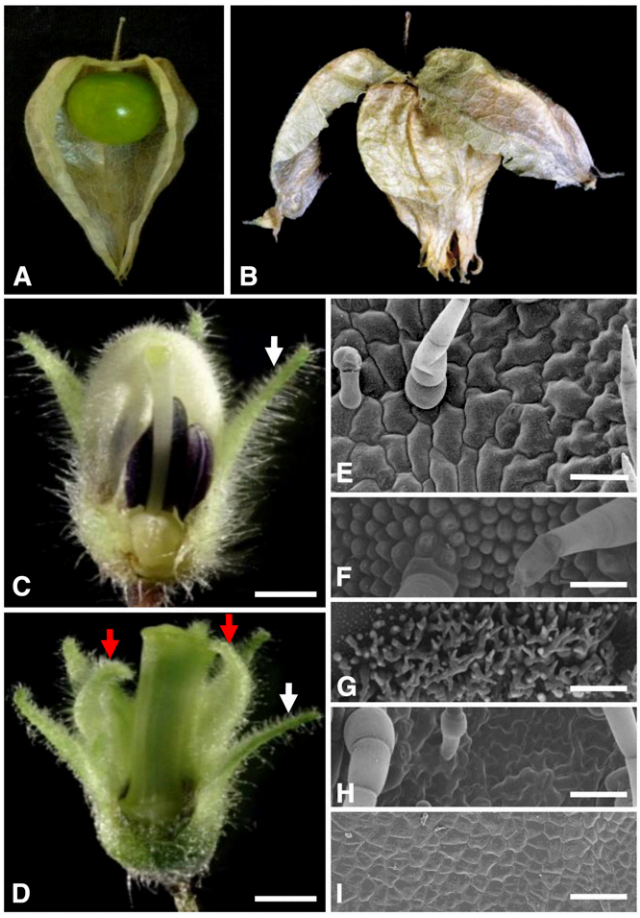

Figure 1. Floral phenotypic analyses of the *doll1* mutant. A, A wild-type fruit. Part of the ICS was removed to show the berry inside. B, A fruit from the *doll1* mutant. The first layer of the lantern was broken to show the second layered lantern. C, A wild-type flower. D, A mutated flower. Parts of the vegetative organs of the flower were removed to show the reproductive structures. White arrows indicate the tip of the calyx, while the red arrows indicate the tip of the transformed calyx in the mutated flower. Bars = 1 mm. E, Epidermal cells on the abaxial zone proximal to the tip of the calyx. F, Epidermal cells on the abaxial tip zone of the corolla from a wild-type flower. G, Epidermal cells on the adaxial base of the corolla from a wild-type flower. H, Epidermal cells on abaxial tip zone of the second whorl of the mutated flower. I, Epidermal cells on adaxial base zone of the second whorl of the mutated flower. Bars = 100 um.

of ICS through the MPF3-MPF2/*MPF2* interaction and regulatory circuit (He et al., 2007; Zhao et al., 2013). Both MPF2 and MPF3 secure their new roles in male fertility through the evolution of novel genetic and physical interactions with the key components for male functionality, for example, the GLOBOSA (GLO) proteins (He and Saedler, 2005; He et al., 2007; Zhao et al., 2013). Thus, the ICS origin is assumed to be associated with fertility, an assertion that is corroborated by the observation that successful fertilization is required for ICS development (He and Saedler, 2005).

Although apparently simple, ICS is actually a complex trait. To delve deep into the molecular origin of this morphological novelty, mutagenesis of *Physalis floridana* via γ-ray radiation was initiated (Lönnig, 2010). One line of an M_2 family (M1750) segregating with floral homeotic transformation was obtained. The mutant featured two homeotic alterations related to the corolla and androecium. Unlike wild-type plants (Fig. 1A), once the berry was set, the mutant featured two whorls of the "Chinese lantern" (Fig. 1B), thus being named the *double-layered-lantern1* (*doll1*) mutant. According to the ABC model of flower development, A functions alone specifies sepal identity, A and B function together to control petal identity, B and C function together to control stamen identity, and C functions alone to specify carpel identity (Coen and Meyerowitz, 1991). We hypothesized that the *doll1* mutant might result from a typical and strong mutation of the B-function MADS-box genes, perhaps like orthologs of the *GLO*/*PISTILLATA* (*PI*) and *DEFICIENS* (*DEF*)/*AP3* genes in *Antirrhinum majus* and Arabidopsis, respectively (Sommer et al., 1990; Jack et al., 1992; Tröbner et al., 1992; Goto and Meyerowitz, 1994; Egea-Cortines et al., 1999; Lamb and Irish, 2003). *GLO* and *DEF* are closely related paralogs, and both gene lineages were duplicated before the ancestor of the core asterids (Hernández-Hernández et al., 2007; Viaene et al., 2009), thus resulting in the GLO1 and GLO2 clades in the GLO lineage and the DEF and TOMATO MADS6 (TM6) clades in the DEF lineage. The two duplicates for each lineage redundantly partitioned the role of the B function with a variable subfunctionalization process in *Petunia hybrida*, *Nicotiana benthamiana*, and *Solanum lycopersicum*. This supposition is supported by the observations that a single mutation in each lineage in a species shows a partially mutated B-type phenotype in these Solanaceous species (Vandenbussche et al., 2004; de Martino et al., 2006; Rijpkema et al., 2006; Geuten and Irish, 2010).

In *Physalis* spp., *GLO* genes are also duplicated, and *PFGLO1* and *PFGLO2* were isolated from *Physalis floridana* (Zhao et al., 2013). As male fertility, the primary function of the androecium, is associated with ICS development (He and Saedler, 2005; He et al., 2007; Zhao et al., 2013), we further assumed that the B-functional genes might have a potential association with the development of the novelty ICS in *Physalis* spp. To empirically address this hypothesis, we here analyzed the *doll1* mutants and characterized B-class MADS-box genes with an emphasis on the functional divergence of the two *GLO* duplicates. We demonstrated that PFGLO1 and PFGLO2 have diverged in terms of their molecular interactions and developmental roles, thus representing a new divergent pattern of the *GLO* duplicates within the Solanaceae. The functional evolution of the *GLO* genes and their potential roles in the development and evolution of the "Chinese lantern" are discussed.

RESULTS

The *doll1* Mutant Features Double-Layered Calyces

The four-whorl floral organs of the wild-type *Physalis floridana* are, from the outer side to the inner side, the

calyx, corolla, androecium, and gynoecium (Fig. 1C). However, in the *doll1* mutant, the corolla was replaced by the calyx and the androecium was replaced by the gynoecium (Fig. 1D). The tip of the outer floral calyx in the wild-type flower and in the mutated flower stretched outward (Fig. 1, C and D, highlighted in white arrows), while the transformed floral calyx in the mutant bent inward (highlighted by red arrows in Fig. 1D), like the tip of the corolla (Fig. 1C). Scanning electronic microscopy (SEM) analyses revealed that in both wild-type and *doll1* mutant plants, the epidermal cells in the zones proximal to the tip of the calyx began to enlarge and became lobate at anthesis. Moreover, the trichomes and stomatal apparatus were developed (Fig. 1E). In wild-type flowers, epidermal cells on the second floral whorl were under differentiated statuses in different zones. In the abaxial tip zone, they were regular dome cells, and trichomes developed occasionally (Fig. 1F), while the adaxial zone proximal to base was covered by extensive and tiny trichomes (Fig. 1G). In contrast to this, the cells on the second floral whorl of the mutant became calyx like, i.e. they were lobate and imbedded with trichomes and stomatal cells (Fig. 1H), while adaxial cells at the base zone, rather than developing the extensive trichomes as on the corolla (Fig. 1G), remained small and undifferentiated (Fig. 1I), like the cells on calyx base (Hu and Saedler, 2007). The epidermal cells on the transformed calyx were significantly deviated from the epidermal cells on the corolla, while actually resembling the cells on the calyx, further supporting that the corolla was transformed into the calyx in the *doll1* mutant. The transformed gynoecium from the androecium was often fused with the original gynoecium in the mutated flower (Fig. 1D). Lacking an androecium, the mutant was male sterile. Once fertilized with wild-type pollen grains, two layers of the "Chinese lantern" were formed in the mutant (Fig. 1B). However, the fruiting rate was less than 2%, hinting that female fertility was also affected in this mutant. We thus assumed that mutations in the B-class MADS-box genes might cause the mutated phenotype, and hence these genes were further investigated in *Physalis floridana*.

Molecular Characterization of *Physalis floridana* B-Class MADS-Box Genes

Six B-class MADS-box gene transcripts were isolated in *Physalis floridana* and named *PFGLO1*, *PFGLO2*, *PFDEF*, *PFTM6*, *PFminiDEFa*, and *PFminiDEFb*. Phylogenetic analyses with multiple methods revealed that these *Physalis floridana* genes fell into one of two groups: the *GLO* or *DEF* lineages (Supplemental Fig. S1; Supplemental Data Set S1). In the Solanaceae, each of these two groups was duplicated during evolution, yielding the *GLO1*- and *GLO2*-like variations in the *GLO* lineage and the *DEF*- and *TM6*-like variations in the *DEF* lineage (Supplemental Fig. S1). Sequencing these genes revealed that *PFGLO1* (3,804 bp), *PFGLO2* (2,299 bp), *PFDEF* (3,685 bp), and *PFTM6* (3,547 bp) had identical structures with seven exons for each gene (Fig. 2A). *PFminDEF* (2,074 bp), which resulted from a duplication of *PFDEF*, encoded the two transcripts *PFminiDEFa* and *PFminiDEFb*, a result of alternative splicing (Supplemental Figs. S1 and S2). Moreover, the structure of *PFminiDEF* was altered dramatically and resulted in an unusual MADS-domain protein (Fig. 2A; Supplemental Fig. S2), indicating that it was very likely a pseudogene.

We also investigated the expression domains of these *Physalis floridana* genes. The results of quantitative reverse transcription (qRT)-PCR analyses demonstrated that transcripts of none of these genes could be detected leaves. *PFGLO1*, *PFGLO2*, and *PFDEF* were predominantly expressed in the corolla and androecium; *PFTM6* was abundantly expressed in the calyx, corolla, and gynoecium (Fig. 2B). Surprisingly, *PFminDEF*, a putative pseudogene, had a similar expression pattern to *PFTM6* (Fig. 2B).

In the *doll1* mutant, *PFGLO1* seemed not to be expressed in flowers, and no *PFGLO1* complementary DNA (cDNA) was obtained, while other B-class MADS-box genes were transcribed as in the wild type (Supplemental Fig. S3A), and the cDNA sequences were identical to these of the wild type. Moreover, genomic fragment of *PFGLO1* was not amplified in the *doll1* mutant (Supplemental Fig. S3B). These analyses suggest that *PFGLO1* might have been deleted from the *doll1* genome, resulting in the nonexpression of this gene.

Floral Expressions of MADS-Box Genes in the Wild Type and the *doll1* Mutants

To further confirm the above notion, the spatial expression of *PFGLO1* and *PFGLO2* during the early floral development was investigated using mRNA in situ hybridization. In the wild type, *PFGLO1* was expressed in the primordium of the corolla and androecium (Fig. 3, A–C). In the *doll1* mutant background, no *PFGLO1* expression signal was detected (Fig. 3, D–F). *PFGLO2* shared an identical expression domain with *PFGLO1* in the wild type (Fig. 3, H–J). However, in the *doll1* mutant, expression of *PFGLO2* was attenuated (Fig. 3, K–M); it was only observed in the primordium of the second whorl (Fig. 3K) and, later on, was restricted to the tip of the transformed calyces (Fig. 3, L and M). Hybridizations with sense probes of *PFGLO1* (Fig. 3G) or *PFGLO2* (Fig. 3N), respectively, were used as the controls. In further qRT-PCR analyses, no *PFGLO1* was detected at all, while *PFGLO2*, *PFDEF*, and *MPF2* were significantly down-regulated in the mutated flowers, *MPF3*, *PFAG* (for an *AGAMOUS* homolog from *Physalis floridana*), and *PFTM6* were significantly up-regulated, and *PFSEP1* (for a *SEPALLATA 1* homolog from *Physalis floridana*) and *PFSEP3* were slightly up-regulated compared with the wild type (Supplemental Fig. S4). These findings confirmed that

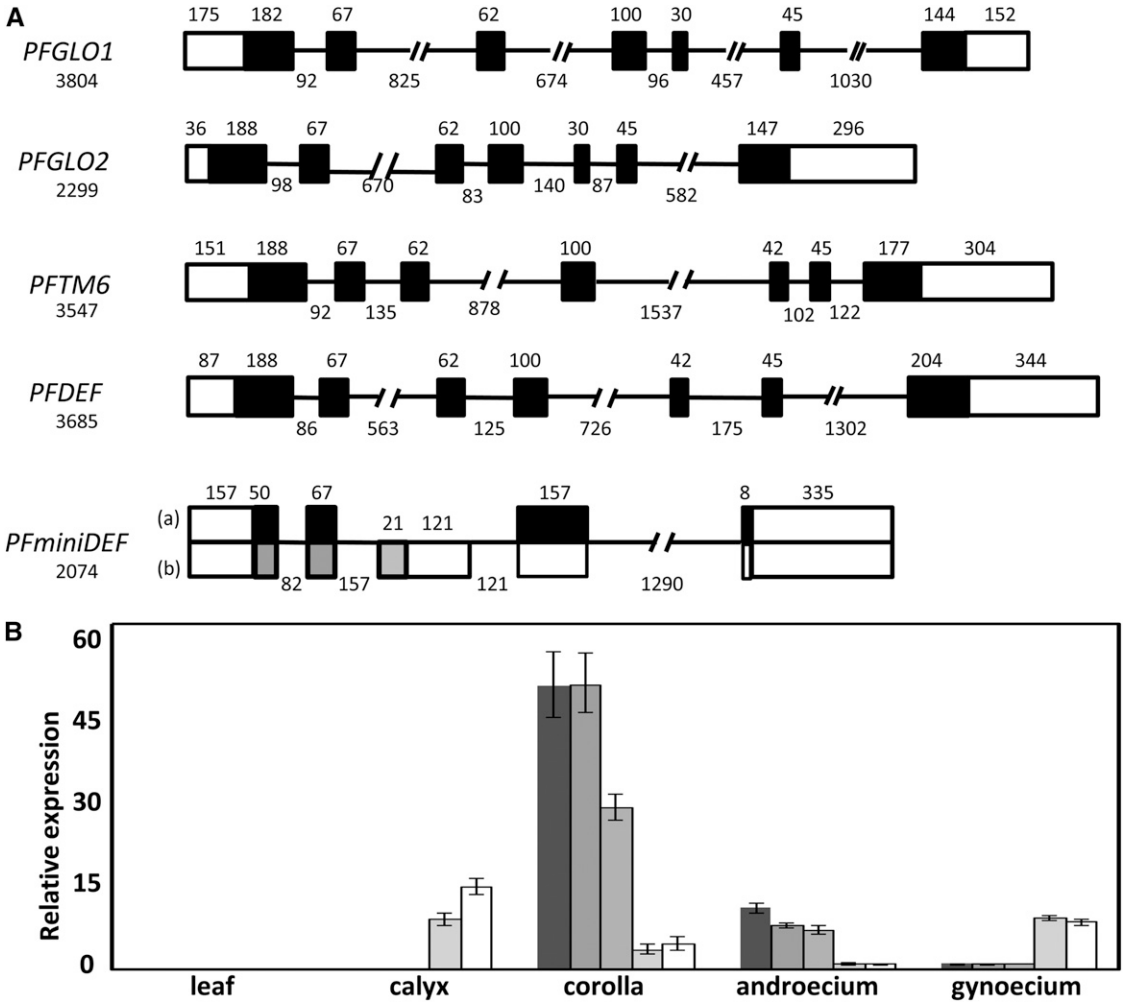

Figure 2. Molecular characterizations of the B-class MADS-box Genes in *Physalis floridana*. A, The exon-intron structure of the B-class MADS-box genes. Five B-class MADS-box genes were obtained. Boxes stand for the exons. Black boxes represent the coding regions, while the empty boxes represent untranslated regions. The lines represent introns. The length of each gene and the size of each intragenic region are given in base pairs. The digit above the box indicates the length of the corresponding exon, while the digits under the line indicate the length of the corresponding intron. For *PFminDEF*, two alternative splicing transcripts, a and b, are shown. B, Relative expression of the B-class MADS-box genes. Expression of *PFGLO1*, *PFGLO2*, *PFDEF*, *PFTM6*, and *PFminDEF* from left to right was investigated via qRT-PCR. *PFACTIN* was used as an internal control. The experiments were repeated three times using three independent biological samples. Mean expression values and SD are presented.

PFGLO1 was not expressed in the *doll1* mutant and suggested that these altered genes might be potential targets of PFGLO1.

The *PFGLO1* Locus, Genetic Segregation, and Genomic Complementation

To understand the nature of *PFGLO1* silencing in the *doll1* mutant, we analyzed the genomic structure of the *PFGLO1* locus. An 18,692-bp-long fragment was assembled in the wild type, including 4,028 bp of upstream and 14,664 bp of downstream sequence (Fig. 4A), if the first nucleotide of *PFGLO1*'s open reading frame (ORF) was defined as position 1. Any fragment between positions –2,998 and 11,970 was not detected in the *doll1* mutant genome, thus the mutant resulted from a large genomic deletion (14,968 bp) harboring *PFGLO1* (Fig. 4A). Gene annotation of the wild-type sequences indicated that no other ORFs linked with *PFGLO1* were found in the large deleted fragment, suggesting that possibly a single gene (*PFGLO1*) was deleted in the mutant.

To genetically link the deletion and the mutated phenotypes, we conducted genetic analyses. The F1 hybrids resulting from pollination of the mutant gynoecium with wild-type pollen grains had the wild-type *Physalis floridana* floral phenotype. The inheritance of the mutated phenotype was evaluated in a total of 693 F2 progeny. The mutated phenotype segregated in a manner consistent with Mendel's law (wild type [519]: mutant [174] = 3:1; $\chi^2 = 0.004$ for 3:1,

P = 0.95; Fig. 4C). Genomic DNA from 598 lines of the segregating population was analyzed for genetic-phenotype linkage analysis using *PFGLO1*-linked molecular markers Primers for Marker1 (PM1) and MP2 (Fig. 4A). The genomic DNA fragments of the expected size could be only amplified from the individuals with wild-type phenotypes (Fig. 4B). These markers cosegregated well with the mutated phenotype; the segregation of the wild type (448) and the mutant (150) was 3:1 (χ^2 = 0.002 for 3:1, P = 0.96; Fig. 4, B and C), indicating that the *doll1* mutant resulted from a monofactorial and recessive mutation with a high likelihood of occurring in the *PFGLO1* locus.

We next transformed a 6,135-bp genomic fragment covering the complete *PFGLO1* locus from the wild type (Fig. 4A) into the F2 progenies and obtained five transgenic plants. Then, we used MP1, MP2 (two markers on the transformed fragment), and MP3 (a marker outside of the transformed fragment) to characterize these transgenic plants. One transgenic plant in the homozygous *doll1* background (*PFGLO1*:*PFGLO1-doll1*-L4) was found, as indicated by the lack of amplification of MP3 (Fig. 4D). Compared with the wild-type flower (Fig. 4E) and the *doll1* flower (Fig. 4F), the mutated phenotype was completely rescued in the *PFGLO1*:*PFGLO1-doll1*-L4 flowers (Fig. 4G). Moreover, the expression of the significantly altered MADS-box genes in the *doll1* mutants (Supplemental Fig. S4) was restored to an equivalent level to that of the wild type by the *PFGLO1*:*PFGLO1* expression (Fig. 4H). Thus, we conclude that the *DOLL1* encodes the PFGLO1 protein. These results also hinted at a functional divergence of PFGLO1 from PFGLO2.

Extensive Variations at Protein Sequences Predict Functional Divergence

Because the expression domains of *PFGLO1* and *PFGLO2* were kept unaltered, the alteration at protein level might likely account for the functional divergence. Sequence comparison revealed that the paralogous protein pair shared 67% identity. The diverged sites (33%) had occurred conservative (amino acid changes with similar physicochemical property) or radical (amino acid changes with different physicochemical property) substitutions during evolution. In total, 70 substituted residues between PFGLO1 and PFGLO2 and 34 radical substitutions were found in the four domains of these MADS-domain proteins (Supplemental Fig. S5). Compared with other Solanaceous GLO orthologous pairs, we found that 25 mutational sites that had radically substituted were clade specific to separate GLO1- and GLO2-like. Moreover, substantial species-specific mutated sites were observed between each paralogous pair (Supplemental Fig. S5). Particularly, L_{18} and I_{163} in the M and K domains of PFGLO2 and P_{61} in the I domain of PFGLO1 were found to be the *Physalis floridana*-specific mutated residues. These domains are

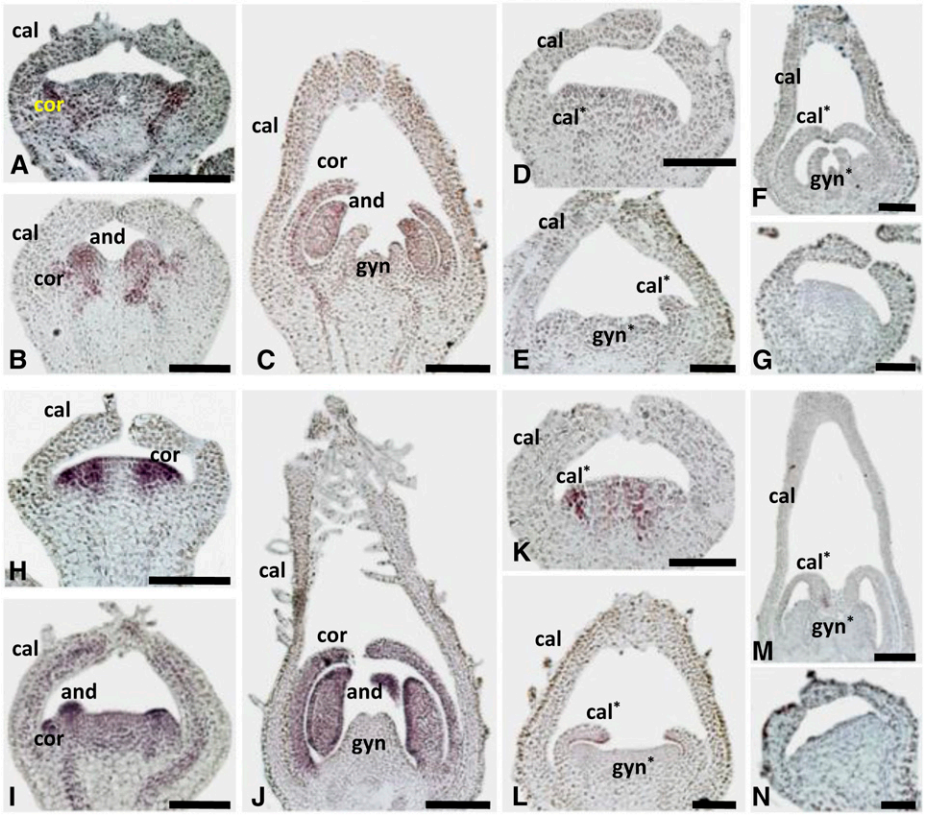

Figure 3. mRNA in situ expression of *PFGLO1* and *PFGLO2*. A to F, Expression of *PFGLO1*. Antisense probe in the wild type (A–C) and in the *doll1* mutant (D–F). G, Sense probe of *PFGLO1*. H to M, Expression of *PFGLO2*. Antisense probe in the wild type (H–J) and in the *doll1* mutant (K–M). N, Sense probe of *PFGLO2*. The primordium of the calyx (cal), corolla (cor), transformed calyx (cal*), androecium (and), gynoecium (gyn), and transformed gynoecium (gyn*) are shown. Asterisk indicates the transformed organ primordium in the *doll1* mutant. Bars = 100 μm.

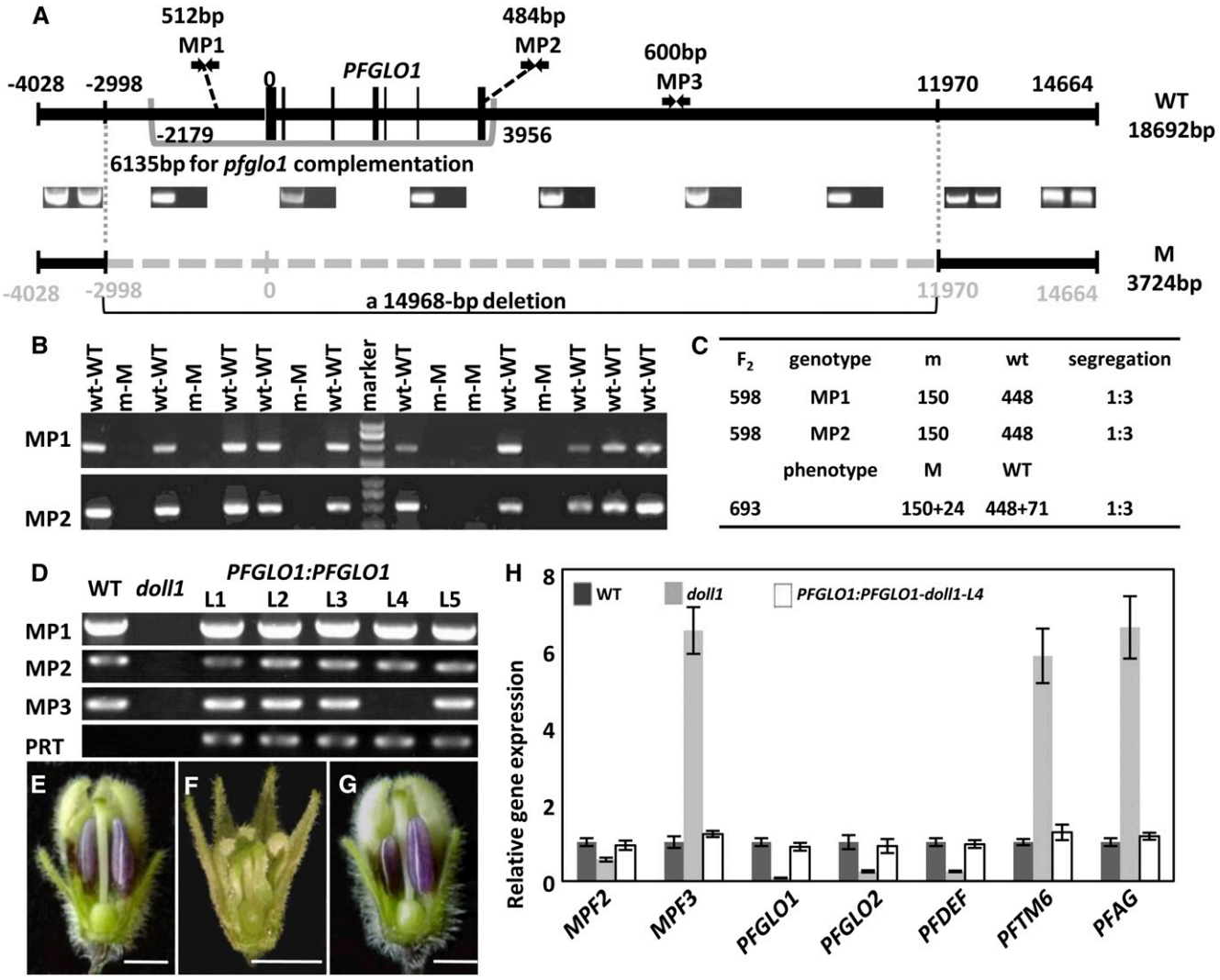

Figure 4. Reconstruction of the *PFGLO1* locus, genetic segregation analysis, and genomic complementation of the *doll1* mutant. A, Reconstruction of the *PFGLO1* locus. Black lines represent the genomic sequences obtained; the dashed line represents the lost sequences in the mutant. The intron-exon structure of *PFGLO1* is shown for the wild type (WT). MP1 and MP2 are two *PFGLO1*-based markers used to screen the homozygous *doll1* mutant. The bracketed region was used for functional complementation in the *doll1* mutant. B, Linkage and cosegregation analyses between the two *PFGLO1*-based markers and the mutated phenotype in the F2 population from a cross of the wild type and the *doll1* mutant. W, Wild type; M, mutant; w, sample with amplified band; m, sample without amplified band. C, Segregation rate of the *PFGLO1*-based markers and mutated phenotypes in the F2 population. D, Generation of transgenic plants harboring *PFGLO1*:*PFGLO1* in the *doll1* mutant. MP1, MP2, and MP3 were amplified in the genomes of the wild type, the *doll1* mutant, and the five transgenic lines (L1, L2, L3, L4, and L5), indicating that L4 is *PFGLO1*:*PFGLO1-doll1* plant. The PRT (primers for the pBAR-vector test) marker from the binary vector was amplified to show the identity of the transgenic plants. E, A wild-type flower. F, A *doll1* flower. G, A *doll1* flower with expression of *PFGLO1* driven by its native promoter (*PFGLO1*:*PFGLO1-doll1*-L4). Part of the calyx and corolla was removed to show the organs inside. Bars = 2.5 mm. H, Relative expression of *PFGLO1* and other MADS-box genes in flowers from wild-type, *doll1*, and *PFGLO1*:*PFGLO1-doll1*-L4 plants. *PFACTIN* was used as an internal control. The expression experiments were repeated three times using independent biological samples. Mean expression values and SD are presented. [See online article for color version of this figure.]

essential in both protein-protein interactions and protein-DNA interactions of the MADS-domain regulatory proteins (Immink et al., 2010). Therefore, the spectrum and specificity of the molecular interaction targets of PFGLO1 and PFGLO2 could be changed, thus leading to different developmental roles. We next investigated their divergence at these various levels.

Virus-Induced Gene Silencing Analyses Reveal Diverged Developmental Roles

We exploited virus-induced gene silencing (VIGS) to dissect the functional divergence of *PFGLO1* and *PFGLO2*. Eight-four of 115 *PFGLO1*-VIGS plants produced similar and visible floral variation. Compared with

the wild type (Fig. 5, A–C), three categories of mutated phenotypes related to homeotic transformation of both corolla and androecium into the calyx and gynoecium (m1, m2, and m3) were observed in these lines (Fig. 5, D–G). *PFGLO1* was knocked down to differing extents in the m1, m2, and m3 flowers (Fig. 5L). The extent of the phenotypic transformation apparently depended on the dose of *PFGLO1* mRNA. In the m1 grade, the androecium was only mutated partially (Fig. 5, D and E), and in the m2 grade, the androecium was completely transformed into a gynoecium, while the corolla was not changed at all (Fig. 5F). The phenotype in the most severe category m3 (Fig. 5G), in which *PFGLO1* expression was only 10% of that observed in the wild type (Fig. 5L), resembled the *doll1* mutant (Fig. 1D). We also found that the expression of *PFGLO2* was attenuated in these *PFGLO1* down-regulated flowers (Fig. 5M), as was observed in the *doll1* mutant.

PFGLO2 was specifically expressed in floral whorl 2 when *PFGLO1* was absent, hinting that PFGLO2 might have a particular role in the development of the second floral whorl. To reveal this, *PFGLO2*-VIGS lines were produced. The results of qRT-PCR analyses showed that the expression of *PFGLO2* was specifically and efficiently knocked down, as evidenced by the fact that *PFGLO2* expression in some flowers was no more than 10% of that seen in the wild type (Supplemental Fig. S6A), while the expression of *PFGLO1* was not affected in these *PFGLO2*-VIGS flowers (Supplemental Fig. S6B), suggesting that *PFGLO1* is not regulated by PFGLO2. Even the most severe down-regulation of *PFGLO2* did not reveal any visible phenotypic variation (Fig. 5, H and I). Pollination with wild-type pollen grains led to normal fruit development, indicating that the functionality of the gynoecium is not impaired. In I_2-KI staining assays, 99.8% of wild-type pollen grains were deeply stained blue (Fig. 5J), while less than 50% of the pollen grains from the *PFGLO2*-VIGS flowers were stained blue. In one extreme case, only 10% of the pollen grains assayed were mature (Fig. 5K). As a negative control, the phytoene desaturase gene from *Physalis floridana*-VIGS flowers developed normal pollens as the wild type (Zhao et al., 2013). Therefore, down-regulation of *PFGLO2* alone did not affect organ identity but may conceivably directly or indirectly block sugar translocation to the pollen, thereby specifically preventing maturation of pollen grains.

Divergent Subcellular Localization and Protein-Protein Interactions

Import into the cell nucleus is critically important for transcription factors to exert their roles. To reveal the subcellular localization of PFGLO1 and PFGLO2, the 35S promoter-driven fusion proteins PFGLO1-GFP and PFGLO2-GFP were produced in *N. benthamiana* leaves. PFGLO1-GFP was mainly observed in the cytoplasm, and if there was any present in the nucleus, it was not highly accumulated (Fig. 6A), while PFGLO2-GFP was mainly detected in the nucleus (Fig. 6B), suggesting different subcellular localizations of the two proteins.

The nuclear import of MADS-domain proteins is often facilitated by formation of homodimers or heterodimers with other MADS-domain proteins (McGonigle et al., 1996; Theissen and Saedler, 2001; Hernández-Hernández et al., 2007). We therefore characterized the interaction of various MADS-domain proteins with both PFGLO1 and PFGLO2. In yeast (*Saccharomyces cerevisiae*), both PFGLO1 and PFGLO2 could not self-activate and formed homodimers, and they were found to have common interacting partners such as MPF3, PFAG, and PFSEP3. In addition, we found that PFDEF interacted with MPF3, PFGLO1, PFAG, and PFSEP3 and that PFTM6 dimerized with MPF3, PFGLO2, PFSEP1, and PFSEP3 (Supplemental Fig. S7). Heterodimerizations of PFGLO1 and PFGLO2 with PFDEF and PFAG were particularly verified in a pull-down assay (Fig. 6C). Glutathione transferase (GST) was fused with both PFGLO1 and PFGLO2 to produce the fusion proteins GST-PFGLO1 and GST-PFGLO2. PFDEF and PFAG, respectively, were labeled with a HIS tag. Western hybridizations using antibodies of HIS (anti-HIS) or GST (anti-GST) confirmed that both PFGLO1 and PFGLO2 interacted with PFAG, while only PFGLO1 maintained the ability to interact with PFDEF.

Heterodimerization of GLO and DEF proteins is essential for their nuclear import and subsequent functions in flower development (Jack et al., 1992; Schwarz-Sommer et al., 1992). The differences in affinity between both PFGLO1/PFGLO2 proteins with PFDEF were further verified with a bimolecular fluorescence complementation (BiFC) assay. In a combination of PFGLO1-YFPNE (for the N-terminal end of YFP) and PFDEF-YFPCE (for the C-terminal end of YFP), the yellow fluorescence protein (YFP) signal was exclusively detected in the nucleus (Fig. 6D), indicating that PFGLO1 and PFDEF interact in the nucleus, further solidifying the notion that the heterodimerization of GLO-DEF is required for their nuclear import, while no YFP signal was observed in the combination of PFGLO2-YFPNE and PFDEF-YFPCE (Fig. 6E), verifying that PFGLO2 and PFDEF do not form heterodimers.

Different Consequences of *PFGLO1* and *PFGLO2* Overexpression in Mutants

To further investigate the divergence, we expressed full-length, 35S promoter-driven cDNAs of *PFGLO1* and *PFGLO2*, respectively, into the *doll1* mutant backgrounds. In total, four lines of *35S:PFGLO1-pfglo1* (1L1–1L4) and six lines of *35S:PFGLO2-pfglo1* (2L1–2L6) were generated (Supplemental Fig. S8). The calyx organ identity of the first floral whorl in all of these transgenic lines was not altered (Fig. 7, A and D). Nonetheless, in the *35S:PFGLO1-pfglo1* lines, the mutated corolla phenotypes were restored, while the inner whorls were further transformed into the corolla-like structure (Fig. 7, B and C), indicating that C function may be strongly

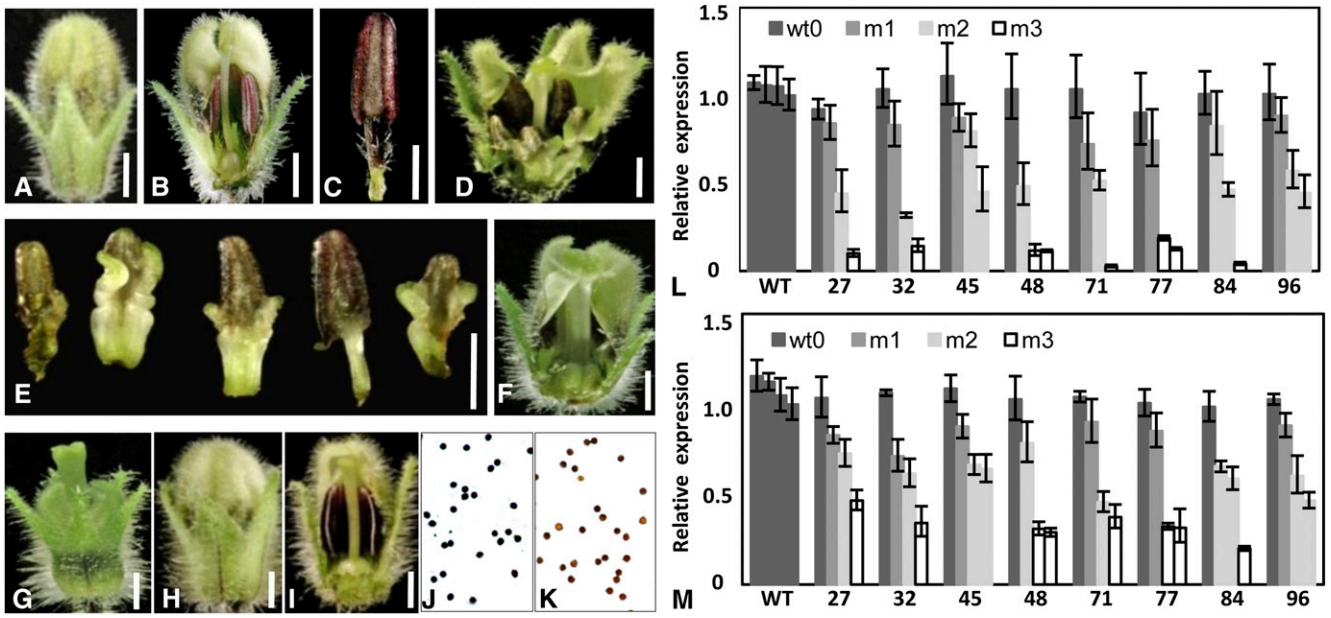

Figure 5. Down-regulating *PFGLO1* in VIGS analyses phenocopies the *doll1* mutant. A, An intact wild-type (WT) flower. B, A dissected wild-type flower to show the androecium and gynoecium. C, A stamen from a wild-type flower. D, A grade m1 flower from the *PFGLO1*-VIGS plants. E, Partially carpel-like androecium from a grade m1 flower. F, A grade m2 flower from the *PFGLO1*-VIGS plants. G, A grade m3 flower from the *PFGLO1*-VIGS plants. H, An intact *pfglo2*-flower from *PFGLO2*-VIGS plants. I, A dissected *pfglo2* flower to show the androecium and gynoecium. Bars = 2 mm. J, I_2-KI-stained pollen from a wild-type flower. K, I_2-KI stained pollen of a *pfglo2* flower from *PFGLO2*-VIGS plants. Active pollen is blue, while sterile pollen is tawny. L, Expression of *PFGLO1* in *PFGLO1*-VIGS flowers. M, Expression of *PFGLO2* in *PFGLO1*-VIGS flowers. Flowers that featured three grades of mutated phenotype (m1, m2, and m3) in eight VIGS-infected lines (27, 32, 45, 48, 71, 77, 84, and 96) were investigated. The expression of MADS-box genes in the wild-type flowers and the wild-type flowers from the VIGS-infected plants (Wt0) were also checked. *PFACTIN* was used as an internal control. The qRT-PCR analyses were repeated three times using independent biological samples. Mean expression values and SD are presented.

repressed. The second floral whorl of the *35S:PFGLO2-pfglo1* lines also had a wild-type-like corolla, but the transformed gynoecia were not altered. Only brown coloration, which is characteristic of the corolla, was seen at the base of the gynoecium (Fig. 7, E and F), indicating that PFGLO2 completely restores the corolla phenotype and does not repress C function.

The repression of C function, putatively exerted by *PFAG* (He et al., 2007; Zhao et al., 2013), was further confirmed via RNA in situ hybridization. In both the wild type and in the *doll1* mutant backgrounds, *PFAG* expression in floral organ primordia was restricted to the inner three whorls (Fig. 7, G and H). However, *PFAG* expression was completely abolished when *PFGLO1* was overexpressed in the *pfglo1* background (Fig. 7I). In the *35S:PFGLO2-pfglo1* transgenic lines, the expression of *PFAG* appeared to be normal (Fig. 7J). No visible signal was seen when the sense *PFAG* probe was used (Fig. 7K).

PFGLO1 and PFGLO2 Evolved Distinct Regulatory Patterns

To reveal more differences in regulatory targets of PFGLO1 and PFGLO2, the expression of the significantly altered MADS-box genes in *doll1* mutant (Supplemental Fig. S5) was investigated in the flowers of both *PFGLO1*-VIGS and *PFGLO2*-VIGS flowers. Three categories of flowers (m1, m2, and m3) from the three *PFGLO1*-VIGS plants (27, 32, and 71) were randomly selected and used to monitor gene expression. The expression tendency of these genes was similar to that in the *doll1* mutant, and the extent of alteration (either up- or down-regulated) apparently depended on the residual *PFGLO1* mRNA levels (Fig. 8A). Similar experiments were performed in the *PFGLO2*-VIGS plants. However, in these *PFGLO2*-down-regulated flowers, the expression of these MADS-box genes was not affected (Fig. 8B). These results suggest that *PFAG*, *PFGLO2*, *PFDEF*, *PFTM6*, *MPF3*, and *MPF2* are direct or indirect target genes of PFGLO1 but that PFGLO2 does not regulate any of these genes. Thus, both genes have evolved distinct regulatory targets and patterns. Because *PFGLO2* became a downstream gene of PFGLO1, the two genes may interact genetically to regulate floral development.

Genetic Interaction of *PFGLO1* and *PFGLO2* in Corolla Development

To reveal genetic interactions, we used a VIGS strategy to produce *PFGLO1PFGLO2* double mutants:

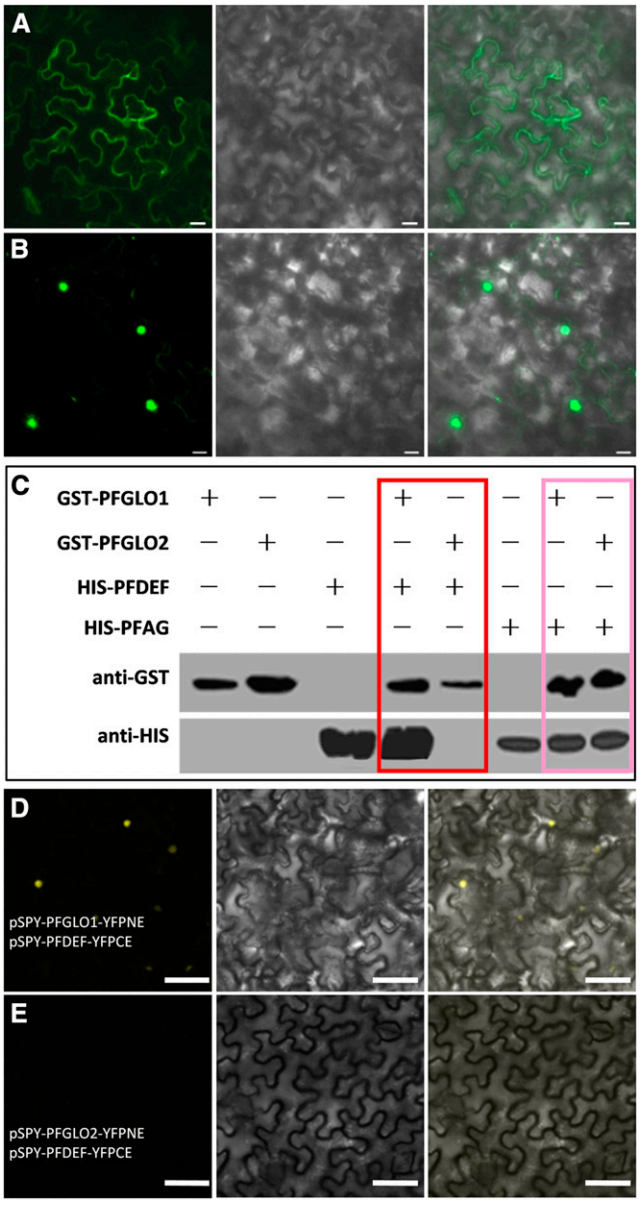

Figure 6. Subcellular localization of PFGLO1 and PFGLO2 and characterizations of their interacting proteins. A and B, Subcellular localization of PFGLO1 and PFGLO2, respectively. From right to left in both A and B are images with green fluorescence, light images, and the merged images. Bars = 20 μm. C, Pull-down assay to confirm that PFGLO1 and PFGLO2 interact with PFDEF and PFAG, respectively. Their interactions with PFDEF are highlighted in the red box, and their interactions with PFAG are highlighted in the pink box. Other lanes are controls. D, PFGLO1 interacts with PFDEF in BiFC. E, Coexpression of PFGLO2-YFPNE and PFDEF-YFPCE. Bars = 50 μm.

PFGLO1-*PFGLO2*-VIGS lines and *PFGLO2*-VIGS-*doll1* (*pfglo1*) lines. Compared with the wild-type flower (Fig. 9A), four categories of mutated phenotypes were seen in the co-VIGS mutated plants (Fig. 9, B–E). Compared with the single mutants (the *doll1* and the most severe *PFGLO1*-VIGS mutated flowers, like in Fig. 9F), there were two different floral phenotypic variations observed in the mutated flowers from the double mutants. The tip of the transformed calyx (the second whorl) in the single *pfglo1* mutant bent inward (highlighted by a red arrow in Fig. 9F), while in the double mutants, i.e. the most severe lines of *PFGLO1*-*PFGLO2*-VIGS (Fig. 9E) and *PFGLO2*-VIGS-*pfglo1* (Fig. 9G), the tip of the second whorl stretched outward or was erected as the calyx developed in the wild type (highlighted by white arrows in Fig. 9A; Fig. 9, E and G). In addition, the organ number in the first and second floral whorls of the wild type and the single mutants was five, while the number of the second floral whorl (the transformed calyx) was increased in the double mutants (Fig. 9H). These phenotypic variations apparently correlated with the degree of cosilencing *PFGLO1* and *PFGLO2* (Fig. 9, I and J). The variation in the expression of the MADS-box genes *MPF3*, *PFAG*, *PFTM6*, and *MPF2* in these double mutants was similar to that observed in the *PFGLO1* mutants (Figs. 8B and 9, I and J). These findings indicate that *PFGLO1* is epistatic to *PFGLO2* and that *PFGLO2* interacts with PFGLO1 genetically to regulate the organ number and the tip development of the second whorl organs.

DISCUSSION

The calyx of *Physalis* spp. inflates to a "Chinese lantern" structure as the berry develops following fertilization. MADS-box genes, such as *MPF2* and *MPF3*, are associated with the evolution and development of this novel structure (He and Saedler, 2005; Zhao et al., 2013). Here, we investigated the *doll1* mutant with the two-layered "Chinese lantern" that resulted from a lack of expression of the *GLO* gene *PFGLO1* in *Physalis floridana*. We found that *PFGLO1*, instead of *PFGLO2*, had its primary role in complete B function, while *PFGLO2* alone exerted a role in male fertility, but controlled the organ number and tip development of the second floral whorl in a *PFGLO1*-dependent manner. Such a diverging pattern of the *GLO* duplicates is distinct from the purely redundant patterns observed in *Petunia hybrida*, *S. lycopersicum*, or *N. benthamiana* (Vandenbussche et al., 2004; Geuten and Irish, 2010).

Functions of the Duplicated *GLO* Genes in *Physalis* spp. Floral Organ Development

The *doll1* mutant resembled the typical mutations in B-function genes from various model plant species. We therefore characterized the closely related B-class homologous genes from *Physalis floridana* and designated as *PFGLO1*, *PFGLO2*, *PFDEF*, *PFTM6*, and *PFminiDEF*. However, the mutant was recessively inherited and resulted from a mutation in one locus. Concomitantly, both expression and locus of *PFGLO1* were not detected. Local genome comparison revealed that a large fragment (about 15 kb) containing *PFGLO1* was deleted from the

genome in this mutant. Genetic linkage analysis further showed that the mutated phenotype closely cosegregated with the loss of *PFGLO1*. Failures in full complementation by *PFGLO1* cDNA indicated that genomic elements like introns might be required for proper gene expression, as described for *ERECTA* (Karve et al., 2011), or overexpressed *PFGLO1* could damage the normal MADS-complex formation. Nonetheless, an approximate 6-kb genomic sequence harboring *PFGLO1* fully complemented the mutated phenotypes, while knocking down *PFGLO1* expression in the wild-type background phenocopied the *doll1* mutant. Thus, we conclude that *DOLL1* encodes the PFGLO1 protein and is dominantly involved in specifying organ identity of the corolla and the androecium in *Physalis floridana*.

These results also imply that the paralogous genes *PFGLO1* and *PFGLO2* might have dramatically diverged in function. In the *doll1* mutant, overexpression of *PFGLO2* cDNA (*35S:PFGLO2-pfglo1*) rescued only the mutated corolla phenotype, while knocking *PFGLO2* down in the wild type did not reveal any visible homeotic variation but inhibited pollen maturation, indicating that PFGLO2 is not necessary in corolla development but is specifically involved in the regulation of male fertility. Nonetheless, PFGLO2 might have retained a potential role in corolla identity but was masked by PFGLO1. Such a complete functional separation of *GLO*-like genes from stamen organ identity was not observed in *Petunia hybrida*, *S. lycopersicum*, or *N. benthamiana* (Vandenbussche et al., 2004; Geuten and Irish, 2010). However, a similar functional separation was observed for the C-class paralogous genes in *Antirrhinum majus*, in which *FARINELLI* (*FAR*) is involved in male fertility, while *PLENA* exerts roles in organ identity specification of the stamen and carpel (Davies et al., 1999).

PFGLO2 had an identical expression domain with *PFGLO1* in the development of the wild-type floral organs. However, in the *doll1* mutant, expression of *PFGLO1* was completely abolished, while *PFGLO2* was expressed in the primordium of the second floral whorl and subsequently restricted to the tip of the transformed organs. When *PFGLO2* was down-regulated, the expression of *PFGLO1* was not affected. These observations suggest that PFGLO1 defines the expression region of and controls the expression level of *PFGLO2* but that PFGLO2 does not regulate the expression of *PFGLO1*. The particular expression domain of *PFGLO2* in the *doll1* suggests that PFGLO2 has a specific role in the development of the second floral whorl and that this role is likely independent of organ identity. The observed physical interactions of PFGLO2 with PFTM6 may be preventing the second floral whorl organs from taking on full calyx morphology because *PFGLO2* was not

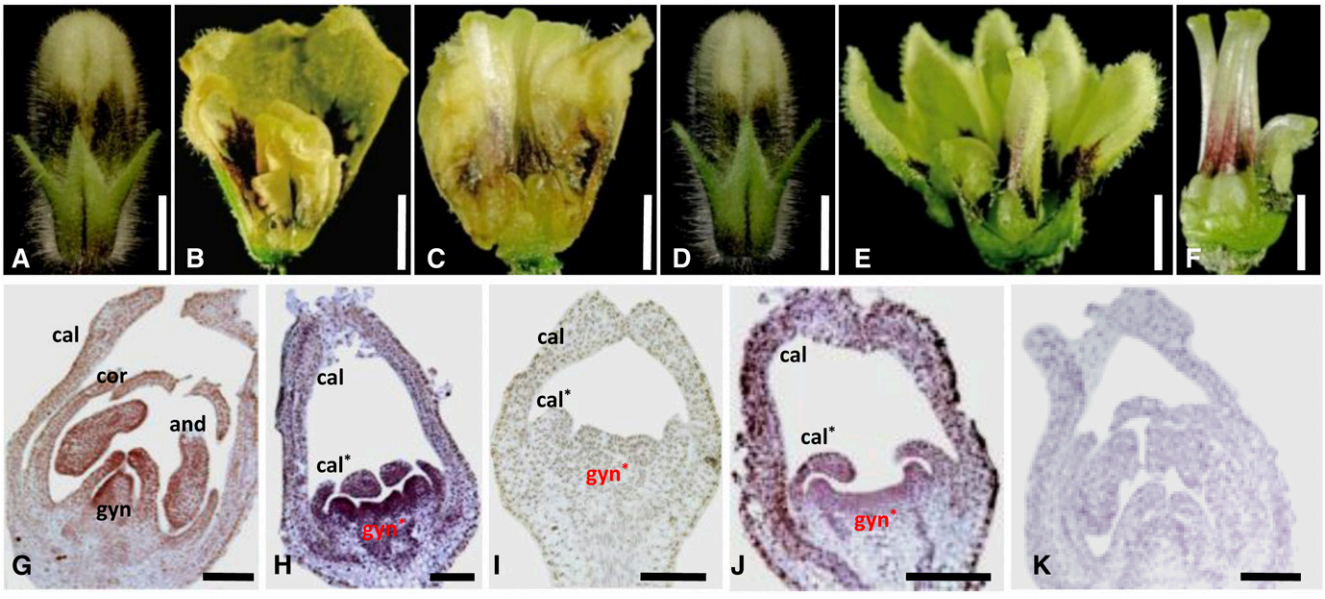

Figure 7. Overexpression further reveals functional divergence. A, A flower bud from a *35S:PFGLO1* overexpression transgenic plant in the *pfglo1* mutant (1L1). B, A flower from a *35S:PFGLO1* overexpression transgenic plant in the *pfglo1* mutant (1L1). The calyx and corolla were partially removed to show the petaloid structure transformed from the reproductive organs. C, The corolla transformed from the gynoecium in *35S:PFGLO1* overexpressed transgenic plants in the *pfglo1* mutant (1L1). D, A flower bud from *35S:PFGLO2* in the *pfglo1* mutant (2L6). E, A flower from *35S:PFGLO2* in the *pfglo1* mutant (2L6). The calyx and corolla were partially removed to show the inner floral organs. F, The transformed fused gynoecium in *35S:PFGLO2* in the *pfglo1* mutant (2L6). Bars = 3 mm. G to J, Expression of *PFAG* revealed by in situ hybridization. Antisense probe of *PFAG* in wild type (G), in the *pfglo1* mutant (H), in *35S:PFGLO1* in *pfglo1* (I), and in *35S:PFGLO2* in *pfglo1* (J). K, Sense probe of *PFAG*. The primordium of the calyx (cal), corolla (cor), transformed calyx (cal*), androecium (and), gynoecium (gyn), and transformed gynoecium (gyn*) are shown. Asterisk indicates the transformed organ primordia in the *doll1* mutant. Bars = 100 μm.

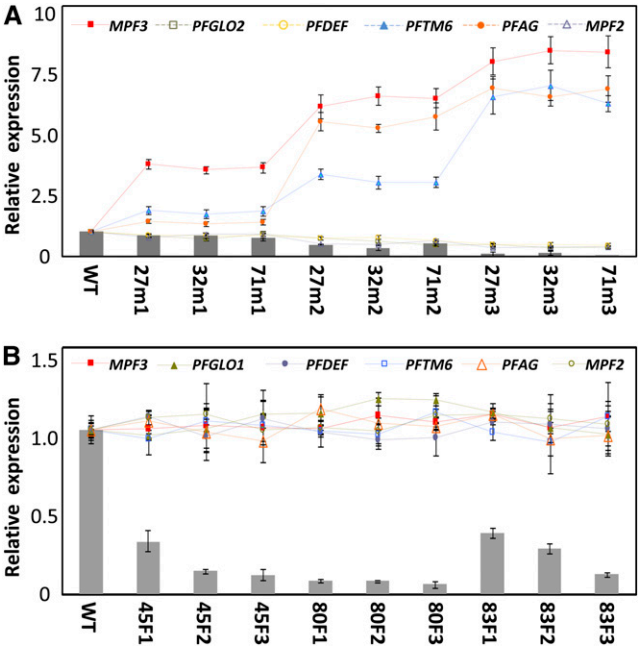

Figure 8. Evolution of distinct regulatory targets and patterns. A, Floral expression of the MADS-box genes in *PFGLO1*-VIGS lines. Flowers that featured three grades of phenotypic variations (m1, m2, and m3) in three VIGS-infected lines (27, 32, and 71) were subjected to qRT-PCR analysis. The experiments were repeated three times using independent biological samples. Mean expression values and SD are presented. B, Floral expression of the MADS-box genes in the *PFGLO2*-VIGS lines. Three flowers (F1, F2, and F3) in three VIGS-infected lines (45, 80, and 83) were subjected to qRT-PCR analysis. The experiments were repeated three times. Mean expression values and SD are presented. In both A and B, the expression of *MPF3*, *PFGLO1*, *PFGLO2*, *PFDEF*, *PFTM6*, *PFAG*, and *MPF2* were compared between wild-type (WT) and mutated flowers. *PFACTIN* was used as an internal control. The columns in A and B represent expression of *PFGLO1* and *PFGLO2*, respectively, while the lines indicate the expression of other genes.

expressed in the calyx but always in the second floral whorl organs, and *PFTM6* was expressed in both calyx and corolla. *PFGLO1PFGLO2* cosilenced mutants gave rise to new phenotypic variations, which were not observed in either the *pfglo1* (*doll1*), *PFGLO1* down-regulated, or *PFGLO2* down-regulated mutants. Thus, *PFGLO2*, genetically interacting with *PFGLO1*, has been restricted to function in the tip development of the second floral whorl prior to anthesis and also functions in controlling the organ number of this floral whorl. The role of PFGLO2 in the tip development might be a residual of corolla organ identity. However, such functional divergence and genetic interaction of two *GLO* genes for the phenotypic determination were not observed in *Petunia hybrida*, *S. lycopersicum*, or *N. benthamiana* (Vandenbussche et al., 2004; Geuten and Irish, 2010).

In *pfglo1*, *MPF3* was significantly up-regulated, thus the new whorl of the calyx developed in place of the corolla. Nonetheless, *MPF3* is expressed in the calyx and the corolla (Zhao et al., 2013), while *PFGLO1* and *PFGLO2* were mainly expressed in the corolla and the androecium. Thus, a direct role of GLO proteins in the development of ICS is unlikely. However, the development of ICS is closely associated with fertility (He and Saedler, 2005, 2007; Zhao et al., 2013). The structural and molecular basis affecting male and female fertility in both *PFGLO2* down-regulated and *doll1* (*pfglo1*) mutants remains elusive. However, fertility seems to be an integral factor for the development of ICS in *Physalis* spp. Maintaining the proper fertility might serve as a strong selective pressure for the evolution of the "Chinese lantern" (He et al., 2007).

Molecular Bases of the Diverged Functions of the *Physalis floridana* GLO Paralogs

MADS-domain regulatory proteins usually form complexes to function in plant development (Theissen and Saedler, 2001; Immink et al., 2010). We discovered that both PFGLO1 and PFGLO2 shared some interacting partners, including MPF3, PFAG, and PFSEP3. MPF3, as an ortholog of AP1 and SQUA, is essential to the calyx development and male fertility (Zhao et al., 2013). PFAG, an ortholog of FAR in *Antirrhinum majus* and AGAMOUS (AG) in Arabidopsis (Bowman et al., 1991; Davies et al., 1999; He et al., 2007), controls male fertility and organ identities of the stamen and the carpel. PFSEP3, a SEPALLATA-like protein, is required for normal floral organ development (Pelaz et al., 2000; He et al., 2007; Immink et al., 2009). However, the direct interactions between B-class proteins and E-class (PFSEP3) proteins were observed in tomato (*Solanum lycopersicum*) but not in Arabidopsis, *Antirrhinum majus*, *Petunia hybrida*, or *Eschscholzia californica* (Davies et al., 1996; Vandenbussche et al., 2004; de Folter et al., 2005; de Martino et al., 2006; Leseberg et al., 2008; Lange et al., 2013), indicating that the dimerization pattern of the homeotic orthologous proteins is variable among angiosperms. However, our findings on protein-protein interactions provide a common basis underlying the role of PFGLO1 and PFGLO2 in floral development in *Physalis floridana*. PFGLO1 interacted with PFAG, PFSEP3, and MPF3 to specify androecium identity, while through these interactions, PFGLO2 was mainly involved in male fertility. Moreover, *TM6*-like genes play roles in carpels, particularly in ovules (de Martino et al., 2006; Geuten and Irish, 2010). We found that *PFTM6*, negatively controlled by PFGLO1, was also expressed in the gynoecium and that its encoding proteins interacted with PFGLO2, MPF3, PFAG, and PFSEP3. These could explain the poor female fertility in the *doll1* mutant. In addition to the roles in fertility, PFGLO1 exerted its full role in the specification of organ identity according to the proposed floral quartets organized by PFGLO1, PFDEF, MPF3, and PFSEP3 in the corolla and those organized by PFGLO1, PFDEF, PFAG, and PFSEP3 in the androecium (He et al., 2007; Theissen and Saedler, 2001). PFGLO2 may fulfill its role in the

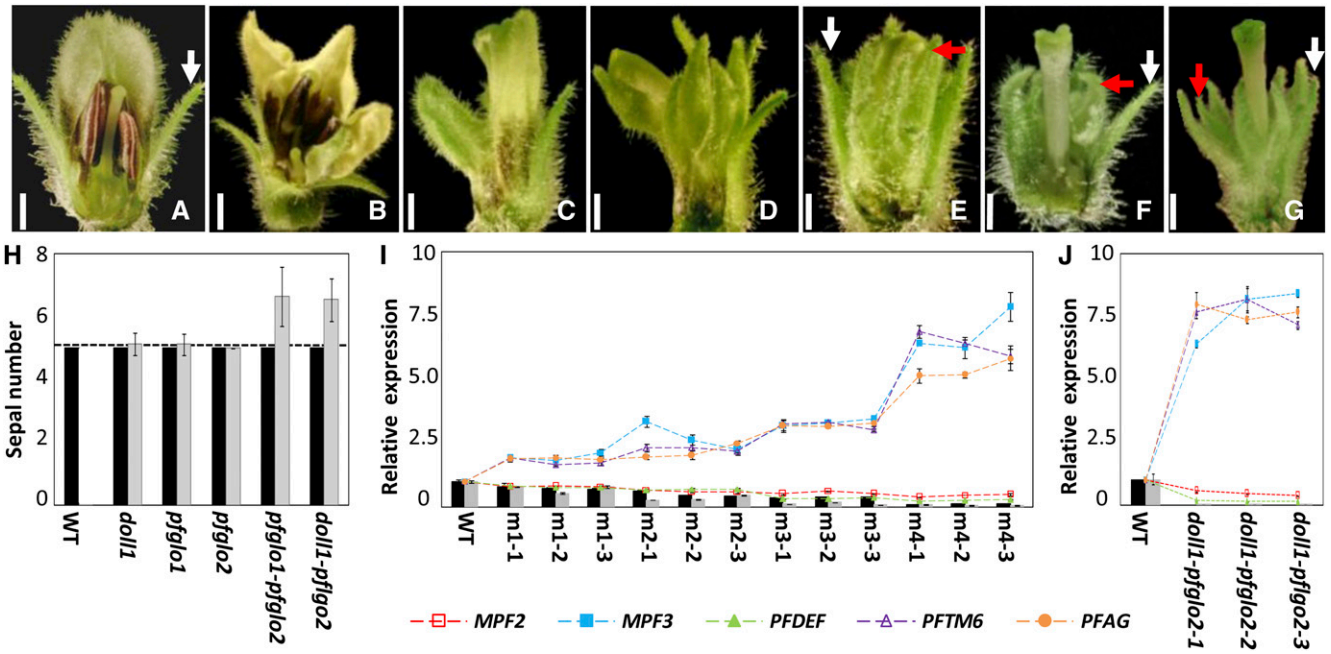

Figure 9. Genetic interaction between *PFGLO1* and *PFGLO2*. A, A wild-type (WT) flower. B to E, Different grades of floral variations m1 (B), m2 (C), m3 (D), and m4 (E) occurred in the double knockdowns of *PFGLO1* and *PFGLO2* via VIGS. F, A flower from the *doll1* mutant. G, A flower from a *PFGLO2*-silencing plant in the *doll1* mutant background. Part of the calyx or the second whorl is removed to show the inside organs. Bars = 2 mm. The white arrows indicate the normal calyx, and the red arrows indicate the transformed calyx. H, The sepal number of the *Physalis floridana*. calyx in various mutant lines, as indicated. Five sepals are typical of the wild-type flowers, as indicated by the dashed line. The black column stands for the original whorl calyx, and the gray column stands for the transformed calyx in the second floral whorl of the various mutants. I, Expression of the MADS-box genes in different grades (m1, m2, m3, and m4) of the double-gene VIGS mutated flowers, as indicated. For each grade, three flowers were collected. J, Expression of MADS-box genes in the double *doll1-pfglo2* mutants. Three mutated flowers were harvested for gene expression. In both I and J, the expression of *MPF3*, *PFGLO1*, *PFGLO2*, *PFDEF*, *PFTM6*, *PFAG*, and *MPF2* were monitored and compared with the wild-type flowers. *PFACTIN* was used as an internal control. Mean expression values and SD are presented.

corolla via a sequestered complex consisting of PFGLO2, MPF3, PFSEP3, PFTM6, and PFDEF. Overexpression of *PFGLO1* or *PFGLO2* restored the mutation in the second floral whorl in the *doll1* mutant, basically confirming the assumptions on their role in corolla. As *PFDEF* was not expressed in the calyx, overexpression of neither *PFGLO1* nor *PFGLO2* produced a double flower, as has been observed in *Tulipa gesneriana* and *Clermontia parviflora*. In later cases, B-class MADS-box genes are heterotopically expressed in the first floral whorl (Kanno et al., 2003; Hofer et al., 2012).

Corroborated with sequence variations, molecular interactions associated with PFGLO1 and PFGLO2 were remarkably diverged. In line with the previous report that simultaneous expression of PI (GLO) and AP3 (DEF) in Arabidopsis is required for their nuclear localization (McGonigle et al., 1996), heterodimerization with PFDEF facilitated the import of PFGLO1 into the nucleus, while PFGLO2 lost the ability to heterodimerize with PFDEF and was likely localized to the nucleus via homodimerization. Furthermore, the petaloid structure was seen when *AG* was mutated in Arabidopsis (Yanofsky et al., 1990; Bowman et al., 1991). This was observed in plants overexpressing *35S:PFGLO1* in the *pfglo1* background, thus suggesting that a C function is repressed by the overexpressed *PFGLO1*. Our expression studies revealed that PFGLO1 repressed *PFAG*, the putative ortholog of *AG* in *Physalis floridana*. A presence of *PFGLO1* genomic fragment in the *doll1* background completely restored both the wild-type floral phenotypes and the expression of all detected MADS-box genes, including *PFAG*. However, our findings are contrary to studies that showed activation of *AG* by AP3 and/or PI in Arabidopsis (Bowman et al., 1991; Wuest et al., 2012) and that demonstrated that the C-function gene *AG2* is reduced in the *seirena1* mutant, a *GLO* mutant in California poppy (*Eschscholzia californica*; Lange et al., 2013). Therefore, transcriptional regulation of *AG* homologs by GLO proteins should be considered to be variable among angiosperms. Moreover, in addition to *PFAG*, we found that PFGLO1 regulates *PFGLO2*, *PFDEF*, *MPF2*, *MPF3*, and *PFTM6*, while PFGLO2 does not regulate any of these genes.

The proposed transcriptional regulations and protein-protein interaction complexes remain to be substantiated functionally. Nonetheless, these findings support

their roles of PFGLO1 and PFGLO2 in flower development, while variations in sequences and molecular interactions may largely explain the observed functional divergence.

Divergent Patterns of the Duplicated *GLO* Genes within the Solanaceae

The auto- and cross-regulatory circuit of obligate heterodimers, such as PI-AP3 in Arabidopsis and GLO-DEF in *Antirrhinum majus*, is required for the specification of petal and stamen identity in angiosperms (Zahn et al., 2005). In the Solanaceae, the circuit is duplicated (Fig. 10); a more complicated but adaptive evolution in the interaction and regulatory networks thus occurred for their functional diversification in flower development (Vandenbussche et al., 2004; Hernández-Hernández et al., 2007; Geuten and Irish, 2010). Divergence is an important strategy in maintaining the duplicated genes (Moore and Purugganan, 2005; Innan and Kondrashov, 2010). *GLO* genes are expressed in the corolla and the androecium (Fig. 10), but the coding sequences of these paralogous regulatory factors dramatically diverged in

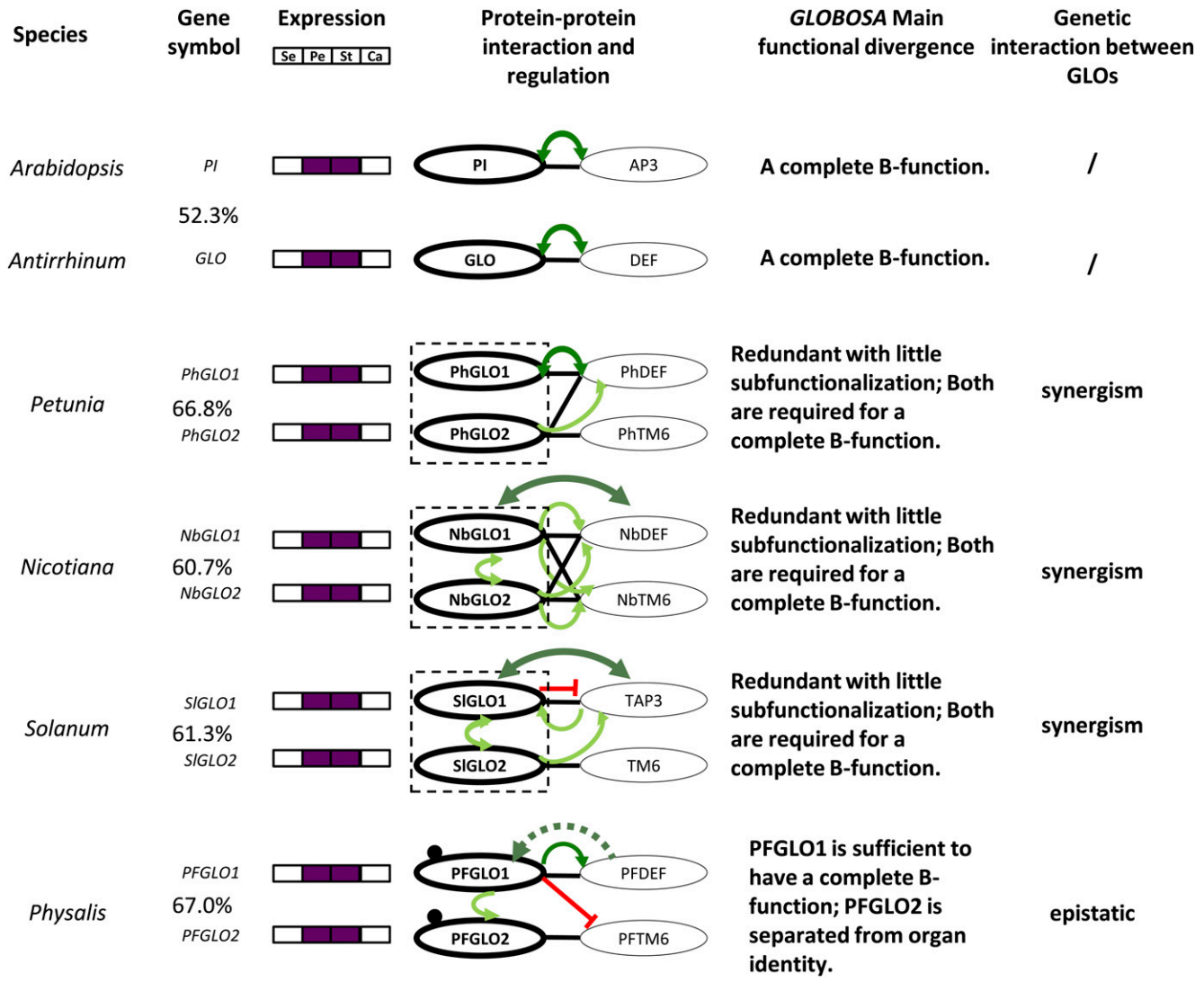

Figure 10. Divergence of the various *GLO* duplicate pairs within the Solanaceae. The protein sequence identity was given between each paralogous pair. In the column of the protein dimerization and regulation, a black line indicates heterodimerization, and a dot near the proteins indicates homodimerization. The curved line with arrows in light green or dark green indicates activation or autoregulation, respectively. The blocked line in red indicates gene repression. The dashed arrow indicated a proposed role needing verification. A dashed box indicates that the two duplicates function as a unit. The functional evolutionary fate and the genetic interaction of each paralogous pair are given. A complete B function is defined as the mutation(s) that could lead to a complete homeotic transformation of the petal and stamen. A slash indicates "no" for this item. Calyx and corolla are homologous to sepals and petals, respectively. For details, please see text. Se, Sepal; Pe, petal; St, stamen; Ca, carpel.

a species (Supplemental Fig. S5). Hence, new protein-protein interactions and novel regulatory roles could be established. Comparisons of these molecular interactions among species could show the evolutionary trajectory of the duplicated paralogous genes (VanderSluis et al., 2010).

While homodimerization was only detected for the GLO proteins in *Physalis floridana*, heterodimer pairs GLO1-DEF and GLO2-TM6 were found to form stably in the Solanaceae (Vandenbussche et al., 2004; de Martino et al., 2006; Rijpkema et al., 2006; Geuten and Irish, 2010); however, maximal cross dimerizations were observed in *N. benthamiana* (Fig. 10). The origin of the specificity of GLO1-DEF and GLO2-TM6 interactions seemed to start from *Petunia hybrida*, and the heterodimer formation became restricted in *S. lycopersicum* and *Physalis floridana* (Fig. 10). Transcriptional regulation of *DEF*-like genes by GLO1-like proteins occurred in all species reported, while the regulation by GLO2-like proteins was observed in *Petunia hybrida*, *N. benthamiana*, and *S. lycopersicum*. The reciprocal autoregulation of the *GLO* duplicates occurs in *N. benthamiana* and *S. lycopersicum*, while in *Physalis floridana*, interestingly, *PFGLO1* is epistatic to *PFGLO2* and activates *PFGLO2* (Fig. 10).

According to the functional consequences of a mutation in either of the GLO (PI)-DEF (AP3) heterodimer pairs, we proposed that both GLO1- and GLO2-like proteins exert their role as a functional unit to bear the complete B function in these species (Fig. 10, highlighted in the dashed box), as the GLO proteins in *Antirrhinum majus* and PI in Arabidopsis do. Moreover, the two *GLO* genes may have a synergistic role in a Solanaceous species. Such subfunctionalization with variability represents an oft-seen diverging pattern of duplicated *GLO* genes, supporting the robustness and evolvability of the B function of the duplicated *GLO* genes (Geuten et al., 2011). However, if one duplicate retains the full B function, another one might deviate from the original developmental program, either becoming lost, as occurred in the basal asterids (Viaene et al., 2009) and in the euasterids I (Lee and Irish, 2011), evolving a new role, or being diverged as happened in *Physalis floridana*.

However, the observed variations in sequences and molecular interactions did not completely explain functional divergence patterns. Extensive sequence alterations between the orthologous pair GLO/PI with a low identity (52.3%) did not change their functions (Fig. 10), hinting a potential role of the coevolution of GLO/PI and DEF/AP3 in the complete B function. In Solanaceous species, the clade-specific mutated sites that originated prespeciation could discriminate the GLO1 and GLO2 clade, while species-specific mutations between the duplicate that occurred after speciation might contribute to the specificity of certain interacting targets, including proteins and DNAs, thus leading to the different developmental consequences. However, similar functional differentiation pattern evolved in *Petunia hybrida*, *N. benthamiana*, and *S. lycopersicum*, where their GLO paralogs respectively shared 66.8%, 60.7%, and 61.3%, while *Physalis floridana*. GLO paralogs (sharing 67% identity) functionally diverged to an extreme extent (Fig. 10). These observations hinted that each GLO paralogous pair might have been under different forces after speciation. The selected formation of GLO1-DEF and GLO2-TM6 during evolution might be the key for functional separation in *Physalis floridana*; however, it did not lead to a significant divergence between the two paralogous pairs in *S. lycopersicum* (Fig. 10). Thus, these findings represent a new functionally divergent pattern of the duplicated *GLO* genes within the Solanaceae. Comparisons in higher order complex formation and complete regulatory networks associated with GLO paralogs among these Solanaceous species will provide further insights into the evolution of these various functional divergence patterns.

MATERIALS AND METHODS

Plant Materials

Physalis floridana P106 (He and Saedler, 2005), the *doll1* (Lönnig, 2010), and their F1 and F2 progenies and transgenic plants were grown in a growth chamber under long-day conditions (16-h/8-h light/dark cycle) with a constant temperature of 22°C. Leaves and floral organs were harvested for genomic DNA or total RNA isolation.

Genome Walking and Gene Annotation

Genome sequences flanking the *PFGLO1* locus in *Physalis floridana* were isolated by rapid amplification of genomic DNA ends (RAGE), using the Universal Genome Walker kit (Clontech). Multiple PCR reactions using genomic DNA from either the *doll1* mutant or wild-type plants as a template were performed to further clarify the obtained sequences. Amplification bands are always expected to appear in the wild type; however, once the amplification bands appeared in both the wild type and mutant, the deletion region in the mutant is thus defined. We used 3,500 bp of upstream sequences and 8,500 bp of downstream sequences of the *PFGLO1* locus ($_{1}$ATG-TAA$_{3956}$) for gene annotation and used the gene prediction program FGENESH (http://linux1.softberry.com/) to search for ORFs. This and similar gene prediction algorithms are typically thought to have rather low accuracy and to yield many false positive results. To preclude these known potential deficiencies from influencing our final conclusions regarding the structure of the deletion, we used the predicted ORFs from FGENESH to search against the sequence database of the Tomato Genome Sequencing Project (http://mips.helmholtz-muenchen.de/plant/tomato/index.jsp), and no homologous sequences were detected. Thus, our gene annotation analysis indicated that no other ORFs were detected in the deleted fragment.

Genetic Linkage Analyses

Homozygous *doll1* plants were pollinated with wild-type pollen to produce F1 seeds, and then F2 seeds were produced through self-fertilization of F1 plants. The phenotype of the F1 plants was identical to that of the wild type. Six hundred ninety-three progeny from F1 plants were grown for segregation analyses. The phenotypes were recorded for each individual in the F2 population. Genomic DNA was isolated from wild-type, *doll1* mutant, and F1 plants and each individual of the F2 population for use in segregation analyses with the *PFGLO1*-linked markers MP1, MP2, and MP3.

RNA in Situ Hybridization

A cDNA fragment covering a portion of the C domain and part of the 3′ untranslated region from each of *PFGLO1* (279 bp), *PFGLO2* (291 bp), or *PFAG* (299 bp) was used as a probe template. Probes were synthesized using the T_7 RNA polymerase driven by a T_7 promoter and labeled with digoxigenin using the DIG RNA Labeling Kit (Roche). Hybridization was performed as described in Carr and Irish (1997), with the alteration that we washed the slides at a temperature of 50°C.

qRT-PCR Analyses

Total RNA was extracted from young floral buds using Plant RNA Reagent (Invitrogen). First-strand cDNA was synthesized with SuperScript III Reverse Transcriptase (Invitrogen) using the Poly (T) primer 5′-CCGGATCCTCTAGAGCGGCCGC $(T)_{17-30}$. qRT-PCR was performed using the SYBR Premix Ex Taq (Perfect Real Time) kit (TaKaRa) according to the manufacturer's manuals of the Mx3000p Real Time System (Stratagene). The amplification conditions were 30 s at 95°C, one cycle, followed by 40 cycles of 5 s at 95°C, and 20 s at 60°C. Data were monitored to detect dissociation curves. *PFACTIN* was used as the housekeeping gene, and relative quantification was performed as previously described (Livak and Schmittgen, 2001).

Yeast Two-Hybrid Assays

ORFs of all MADS-box genes in this study were cloned in frame into the pGADT7 and pGBKT7 vectors (Clontech). The bait and prey construct combinations were cotransformed into the AH109 yeast (*Saccharomyces cerevisiae*) strain and plated on the synthetic dextrose/-Leu-His plates. Then the survived cells were spotted on selective medium (synthetic dextrose/-Leu-His-Trp) supplemented with 3.0 mM 3-amino-1, 2, 4-triazole. The plates were incubated at 28°C for 2 to 5 d.

Pull-Down Assays

ORFs of *PFDEF* and *PFAG* were cloned into the pET-30a (+) vector (containing 6× His tag), expressed in *Escherichia coli* strain BL21 (DE3), and then purified on Ni Sepharose columns (GE Healthcare). ORFs of *PFGLO1* and *PFGLO2* were cloned into the pGEX-4T-1 vector (containing GST tag), expressed in *E. coli* strain BL21, and then infused onto Glutathione Sepharose columns (GE Healthcare). The purified recombinant proteins HIS-PFDEF and HIS-PFAG were mixed into the Glutathione Sepharose columns containing the GST-PFGLO1 or GST-PFGLO2 recombinant proteins, respectively, the columns were washed four times with binding buffer, and the bound proteins were eluted with washing buffer. The eluted proteins were heated and then separated on 12% (w/v) SDS polyacrylamide gels. Proteins were blotted onto nitrocellulose filter membranes (Cwbiotech) using the semidry electrophoretic transfer method, and then the membranes were blocked with 5% (w/v) bovine serum albumin-Tris-buffered saline plus Tween 20 buffer for 1 h. The membranes were initially incubated with anti-GST or anti-HIS antibodies for 2 h, and then anti-HRP antibodies were used as the secondary antibodies for a 1-h incubation. Following each round of incubation, the membranes were washed three times with Tris-buffered saline plus Tween 20 buffer. Radioautographs of the membranes were obtained using Kodak film at room temperature for 1 min and fixed according to standard procedures.

Transient Protein Expression Assays

For subcellular localization studies, the ORFs of *PFGLO1* and *PFGLO2* were cloned into the Super1300 expression vector (Chen et al., 2009) using the *Xba*I/*Kpn*I (Roche) restriction sites and fused to GFP. For the BiFC assays, the ORFs of *PFGLO1*, *PFGLO2*, and *PFDEF* were cloned into the *pSPYNE-35S* and *pSPYCE-35S* vector pair (Walter et al., 2004) using the *Xba*I/*Bam*HI (Roche) restriction sites. These paired vectors were designed to express either the N- or C-terminal halves of YFP. The recombinant constructs of PFGLO1-GFP and PFGLO2-GFP and the construct combination of two proteins fused with the N- or C-terminal halves of YFP were transformed into *Agrobacterium tumefaciens* and were then injected into leaf epidermal cells of *Nicotiana benthamiana* (Walter et al., 2004). Forty-eight hours after injection, the fluorescence signal of the GFP or YFP was detected using a confocal laser scanning microscope (Olympus FV1000MPE).

VIGS, Plant Transformation, and Genotyping

VIGS procedures were performed according to previously described methods (Zhang et al., 2013). A 479-bp cDNA fragment of *PFGLO1*, a 416-bp cDNA fragment of *PFGLO2*, and their respective chimerical fragments were transformed into the tobacco rattle virus vector2 binary vector for the creation of VIGS constructs for both single and double gene silencing. Full-length cDNAs of *PFGLO1* and *PFGLO2* were cloned into the pBAR plant binary vector for overexpression analysis. A 6-kb genomic DNA sequence consisting of the *PFGLO1* locus was also cloned into pBAR for complementation analysis. As no seed from the homozygous mutant was produced, each construct was transformed into F2 progenies from a heterozygous mutant line. The LBA4404 strain of *Agrobacterium tumefaciens* was used for the *Physalis floridana* transformation. The media and transformation procedures used here were identical to previously described methods (He and Saedler, 2005). The transgenic plants were genotyped via various analyses of the PCR using genomic DNA as the template and routine reverse transcription-PCR. The gene silencing in VIGS-infected flowers was confirmed using qRT-PCR analysis.

Morphological Analyses

For SEM analyses, fresh materials were fixed in formalin-acetic-alcohol solution (95% ethyl alcohol:glacial acetic acid:formaldehyde [8:1:1]), sputter coated with gold, and examined with a digital scanning microscope (Hitachi S–4800). Pollen maturation was detected using I_2-KI staining. The floral buds, mature flowers, androecium, and pollen grains were photographed using a Zeiss microscope.

Phylogenetic Reconstructions

BLAST searches were performed in the National Center for Biotechnology Information Blast Suite (http://www.ncbi.nlm.nih.gov/) using the *Physalis floridana* B-class MADS-box genes isolated as queries. Information for all of the sequences downloaded from the National Center for Biotechnology Information database is available in Supplemental Table S1. Coding sequences were aligned as Supplemental Data Set S1 using MEGA5 (Tamura et al., 2011) and manually adjusted in BioEdit version 7.0.9 (Hall, 1999). The Bayesian inference, maximum likelihood, and neighbor-joining phylogeny trees were constructed using protein sequences. The maximum likelihood tree was constructed using the PhyML v3.0 program (Guindon and Gascuel, 2003) under the Jones, Taylor, and Thornton model (bootstrap, 100; γ distribution parameter, estimated). The neighbor-joining tree was constructed with MEGA5 (Kimura two-parameter model; bootstrap, 100; Tamura et al., 2011), and the Bayesian inference tree was generated with MrBayes version 3.1.2 (Huelsenbeck and Ronquist, 2001; prset aamodelpr = mixed; ngen = 1,000,000; samplefreq = 100).

Sequencing Analyses

The 3′ and 5′ cDNA ends of the B-class MADS-box genes from *Physalis floridana*. were amplified according to the standard manual of the 3′/5′ RACE kit (Roche). All sequences were amplified using the TaKaRa LA Taq Polymerase. Amplified fragments were then cloned into the pGEM T-Easy Vector (Promega). All constructs made were commercially sequenced by Beijing Genomics Institute. Primer information used is available in Supplemental Table S2. The sequences reported in this study were deposited in the National Center for Biotechnology Information database under the following accession numbers: JX467691 (*PFGLO1*), KC174706 (*PFGLO2*), KC174703 (*PFDEF*), KC174704 (*PFTM6*), and KC174705 (*PFminDEF*).

Supplemental Data

The following materials are available in the online version of this article.

Supplemental Figure S1. Phylogenetic analyses of B-class MADS-box genes.

Supplemental Figure S2. Genomic loci and their gene products differ between *PFDEF* and *PFminiDEF*.

Supplemental Figure S3. Existence of B-class MADS-box genes in the *doll1* mutant.

Supplemental Figure S4. Floral expression of some MADS-box genes in the wild type and the *doll1* mutant.

Supplemental Figure S5. Pairwise comparison of the GLO paralogous MADS-domain proteins.

Supplemental Figure S6. Expression of *PFGLO* genes in *PFGLO2*-tobacco rattle virus vector2-infected flowers.

Supplemental Figure S7. Protein-protein interactions of *Physalis floridana* MADS-domain proteins in yeast.

Supplemental Figure S8. Genotyping analyses of *PFGLO* genes' overexpressors in the *doll1* mutant.

Supplemental Table S1. B-class MADS-box genes for phylogenetic analyses.

Supplemental Table S2. Primer information used in this work.

Supplemental Data Set S1. Alignment of B-class MADS-domain proteins for phylogenetic analysis.

ACKNOWLEDGMENTS

We thank Dr. Wolf-Ekkehard Lönnig for generously offering the *doll1* mutant seeds and the double-lantern picture (Fig. 1B), Yinhou Xiao for SEM analyses, and Dr. Jingquan Li for operation of the confocal laser scanning microscopic analyses.

Received November 25, 2013; accepted January 2, 2014; published January 3, 2014.

LITERATURE CITED

Bowman JL, Drews GN, Meyerowitz EM (1991) Expression of the *Arabidopsis* floral homeotic gene *AGAMOUS* is restricted to specific cell types late in flower development. Plant Cell **3:** 749–758

Carr SM, Irish VF (1997) Floral homeotic gene expression defines developmental arrest stages in *Brassica oleracea* L. vars. *botrytis* and *italica*. Planta **201:** 179–188

Chen YF, Li LQ, Xu Q, Kong YH, Wang H, Wu WH (2009) The WRKY6 transcription factor modulates *PHOSPHATE1* expression in response to low Pi stress in *Arabidopsis*. Plant Cell **21:** 3554–3566

Coen ES, Meyerowitz EM (1991) The war of the whorls: genetic interactions controlling flower development. Nature **353:** 31–37

Davies B, Egea-Cortines M, de Andrade Silva E, Saedler H, Sommer H (1996) Multiple interactions amongst floral homeotic MADS box proteins. EMBO J **15:** 4330–4343

Davies B, Motte P, Keck E, Saedler H, Sommer H, Schwarz-Sommer Z (1999) *PLENA* and *FARINELLI*: redundancy and regulatory interactions between two *Antirrhinum* MADS-box factors controlling flower development. EMBO J **18:** 4023–4034

de Folter S, Immink RG, Kieffer M, Parenicová L, Henz SR, Weigel D, Busscher M, Kooiker M, Colombo L, Kater MM, et al (2005) Comprehensive interaction map of the *Arabidopsis* MADS Box transcription factors. Plant Cell **17:** 1424–1433

de Martino G, Pan I, Emmanuel E, Levy A, Irish VF (2006) Functional analyses of two tomato *APETALA3* genes demonstrate diversification in their roles in regulating floral development. Plant Cell **18:** 1833–1845

Egea-Cortines M, Saedler H, Sommer H (1999) Ternary complex formation between the MADS-box proteins SQUAMOSA, DEFICIENS and GLOBOSA is involved in the control of floral architecture in *Antirrhinum majus*. EMBO J **18:** 5370–5379

Freeling M, Thomas BC (2006) Gene-balanced duplications, like tetraploidy, provide predictable drive to increase morphological complexity. Genome Res **16:** 805–814

Geuten K, Irish V (2010) Hidden variability of floral homeotic B genes in Solanaceae provides a molecular basis for the evolution of novel functions. Plant Cell **22:** 2562–2578

Geuten K, Viaene T, Irish VF (2011) Robustness and evolvability in the B-system of flower development. Ann Bot (Lond) **107:** 1545–1556

Goto K, Meyerowitz EM (1994) Function and regulation of the *Arabidopsis* floral homeotic gene *PISTILLATA*. Genes Dev **8:** 1548–1560

Guindon S, Gascuel O (2003) A simple, fast, and accurate algorithm to estimate large phylogenies by maximum likelihood. Syst Biol **52:** 696–704

Hall TA (1999) BioEdit: a user-friendly biological sequence alignment editor and analysis program for Windows 95/98/NT. Nucleic Acids Symp Ser **41:** 95–98

He CY, Saedler H (2005) Heterotopic expression of *MPF2* is the key to the evolution of the Chinese lantern of *Physalis*, a morphological novelty in Solanaceae. Proc Natl Acad Sci USA **102:** 5779–5784

He CY, Saedler H (2007) Hormonal control of the inflated calyx syndrome, a morphological novelty, in *Physalis*. Plant J **49:** 935–946

He CY, Sommer H, Grosardt B, Huijser P, Saedler H (2007) PFMAGO, a MAGO NASHI-like factor, interacts with the MADS-domain protein MPF2 from *Physalis floridana*. Mol Biol Evol **24:** 1229–1241

Hernández-Hernández T, Martínez-Castilla LP, Alvarez-Buylla ER (2007) Functional diversification of B MADS-box homeotic regulators of flower development: adaptive evolution in protein-protein interaction domains after major gene duplication events. Mol Biol Evol **24:** 465–481

Hofer KA, Ruonala R, Albert VA (2012) The double-corolla phenotype in the Hawaiian lobelioid genus *Clermontia* involves ectopic expression of *PISTILLATA* B-function MADS box gene homologs. Evodevo **3:** 26

Hu JY, Saedler H (2007) Evolution of the inflated calyx syndrome in Solanaceae. Mol Biol Evol **24:** 2443–2453

Huelsenbeck JP, Ronquist F (2001) MRBAYES: Bayesian inference of phylogenetic trees. Bioinformatics **17:** 754–755

Huijser P, Klein J, Lönnig WE, Meijer H, Saedler H, Sommer H (1992) *Bracteomania*, an inflorescence anomaly, is caused by the loss of function of the MADS-box gene *squamosa* in *Antirrhinum majus*. EMBO J **11:** 1239–1249

Immink RG, Tonaco IA, de Folter S, Shchennikova A, van Dijk AD, Busscher-Lange J, Borst JW, Angenent GC (2009) *SEPALLATA3*: the 'glue' for MADS box transcription factor complex formation. Genome Biol **10:** R24

Immink RG, Kaufmann K, Angenent GC (2010) The 'ABC' of MADS domain protein behaviour and interactions. Semin Cell Dev Biol **21:** 87–93

Innan H, Kondrashov F (2010) The evolution of gene duplications: classifying and distinguishing between models. Nat Rev Genet **11:** 97–108

Irish VF, Litt A (2005) Flower development and evolution: gene duplication, diversification and redeployment. Curr Opin Genet Dev **15:** 454–460

Jack T, Brockman LL, Meyerowitz EM (1992) The homeotic gene *APETALA3* of *Arabidopsis thaliana* encodes a MADS box and is expressed in petals and stamens. Cell **68:** 683–697

Kanno A, Saeki H, Kameya T, Saedler H, Theissen G (2003) Heterotopic expression of class B floral homeotic genes supports a modified ABC model for tulip (*Tulipa gesneriana*). Plant Mol Biol **52:** 831–841

Karve R, Liu W, Willet SG, Torii KU, Shpak ED (2011) The presence of multiple introns is essential for *ERECTA* expression in *Arabidopsis*. RNA **17:** 1907–1921

Lamb RS, Irish VF (2003) Functional divergence within the *APETALA3/PISTILLATA* floral homeotic gene lineages. Proc Natl Acad Sci USA **100:** 6558–6563

Lange M, Orashakova S, Lange S, Melzer R, Theißen G, Smyth DR, Becker A (2013) The *seirena* B class floral homeotic mutant of California poppy (*Eschscholzia californica*) reveals a function of the enigmatic PI motif in the formation of specific multimeric MADS domain protein complexes. Plant Cell **25:** 438–453

Lee HL, Irish VF (2011) Gene duplication and loss in a MADS box gene transcription factor circuit. Mol Biol Evol **28:** 3367–3380

Leseberg CH, Eissler CL, Wang X, Johns MA, Duvall MR, Mao L (2008) Interaction study of MADS-domain proteins in tomato. J Exp Bot **59:** 2253–2265

Livak KJ, Schmittgen TD (2001) Analysis of relative gene expression data using real-time quantitative PCR and the $2^{-\Delta\Delta C_T}$ method. Methods **25:** 402–408

Lönnig WE (2010) Mutagenesis in *Physalis pubescens* L. ssp. *floridana*: some further research on Dollo's law and the law of recurrent variation. Floriculture Ornamental Biotech **4:** 1–21

Mandel MA, Gustafson-Brown C, Savidge B, Yanofsky MF (1992) Molecular characterization of the *Arabidopsis* floral homeotic gene *APETALA1*. Nature **360:** 273–277

McGonigle B, Bouhidel K, Irish VF (1996) Nuclear localization of the *Arabidopsis APETALA3* and *PISTILLATA* homeotic gene products depends on their simultaneous expression. Genes Dev **10:** 1812–1821

Moore RC, Purugganan MD (2005) The evolutionary dynamics of plant duplicate genes. Curr Opin Plant Biol **8:** 122–128

Pelaz S, Ditta GS, Baumann E, Wisman E, Yanofsky MF (2000) B and C floral organ identity functions require *SEPALLATA* MADS-box genes. Nature **405:** 200–203

Rijpkema AS, Royaert S, Zethof J, van der Weerden G, Gerats T, Vandenbussche M (2006) Analysis of the *Petunia TM6* MADS box gene reveals functional divergence within the *DEF/AP3* lineage. Plant Cell **18:** 1819–1832

Schwarz-Sommer Z, Hue I, Huijser P, Flor PJ, Hansen R, Tetens F, Lönnig WE, Saedler H, Sommer H (1992) Characterization of the *Antirrhinum* floral homeotic MADS-box gene *deficiens*: evidence for DNA binding and autoregulation of its persistent expression throughout flower development. EMBO J **11:** 251–263

Sommer H, Beltrán JP, Huijser P, Pape H, Lönnig WE, Saedler H, Schwarz-Sommer Z (1990) *Deficiens*, a homeotic gene involved in the control of flower morphogenesis in *Antirrhinum majus*: the protein shows homology to transcription factors. EMBO J **9:** 605–613

Tamura K, Peterson D, Peterson N, Stecher G, Nei M, Kumar S (2011) MEGA5: molecular evolutionary genetics analysis using maximum likelihood, evolutionary distance, and maximum parsimony methods. Mol Biol Evol **28:** 2731–2739

Theissen G, Saedler H (2001) Plant biology. Floral quartets. Nature **409:** 469–471

Tröbner W, Ramirez L, Motte P, Hue I, Huijser P, Lönnig WE, Saedler H, Sommer H, Schwarz-Sommer Z (1992) *GLOBOSA*: a homeotic gene which interacts with *DEFICIENS* in the control of *Antirrhinum* floral organogenesis. EMBO J **11:** 4693–4704

Vandenbussche M, Zethof J, Royaert S, Weterings K, Gerats T (2004) The duplicated B-class heterodimer model: whorl-specific effects and complex genetic interactions in *Petunia hybrida* flower development. Plant Cell **16:** 741–754

VanderSluis B, Bellay J, Musso G, Costanzo M, Papp B, Vizeacoumar FJ, Baryshnikova A, Andrews B, Boone C, Myers CL (2010) Genetic interactions reveal the evolutionary trajectories of duplicate genes. Mol Syst Biol **6:** 429

Viaene T, Vekemans D, Irish VF, Geeraerts A, Huysmans S, Janssens S, Smets E, Geuten K (2009) *Pistillata*—duplications as a mode for floral diversification in (Basal) asterids. Mol Biol Evol **26:** 2627–2645

Walter M, Chaban C, Schütze K, Batistic O, Weckermann K, Näke C, Blazevic D, Grefen C, Schumacher K, Oecking C, et al (2004) Visualization of protein interactions in living plant cells using bimolecular fluorescence complementation. Plant J **40:** 428–438

Wuest SE, O'Maoileidigh DS, Rae L, Kwasniewska K, Raganelli A, Hanczaryk K, Lohan AJ, Loftus B, Graciet E, Wellmer F (2012) Molecular basis for the specification of floral organs by APETALA3 and PISTILLATA. Proc Natl Acad Sci USA **109:** 13452–13457

Yanofsky MF, Ma H, Bowman JL, Drews GN, Feldmann KA, Meyerowitz EM (1990) The protein encoded by the *Arabidopsis* homeotic gene *agamous* resembles transcription factors. Nature **346:** 35–39

Zahn LM, Leebens-Mack J, DePamphilis CW, Ma H, Theissen G (2005) To B or Not to B a flower: the role of *DEFICIENS* and *GLOBOSA* orthologs in the evolution of the angiosperms. J Hered **96:** 225–240

Zhang JS, Zhao J, Zhang SH, He CY (2014) Efficient gene silencing mediated by tobacco rattle virus in an emerging model plant *Physalis*. PLoS ONE **9:** e85534

Zhao J, Tian Y, Zhang JS, Zhao M, Gong PC, Riss S, Saedler R, He CY (2013) The euAP1 protein MPF3 represses *MPF2* to specify floral calyx identity and displays crucial roles in Chinese lantern development in *Physalis*. Plant Cell **25:** 2002–2021